Technical Session – Mineral Resources Technology

Table of Contents

Oral Session

Poster Session

Investigation on Structural Modification of Sri Lankan Vein Graphite for Ion Intercalation

A.G.T.R.Amiyangoda,

Faculty of Science and Technology, Uva Wellassa University of Sri Lanka and Institute of Fundamental Studies, Kandy, Sri Lanka

and

R.M.N.M. Rathnayake, R.I.C.N. Karunarathne, H.W.M.A.C.Wijayasinghe
Institute of Fundamental Studies, Kandy, Sri Lanka

Introduction

Rechargeable batteries have become the main energy source for the portable electronic devices. Synthetic graphite have been used as anode electrode material in rechargeable batteries. Presently these rechargeable batteries are expensive mainly due to high cost of materials, such as synthetic graphite and metal oxides, used in their electrodes. It is suggested that the cost of these batteries can be reduce by introducing cheaper natural graphite for their anode electrode. Sri Lankan natural vein graphite can be classified into four distinct structural verities. They are Shiny-Slippery-Fibrous Graphite (SSF), Needle-Platy Graphite (NPG), Coarse Striated-Flaky Graphite (CSF) and Coarse Flakes of Radial Graphite (CFR). Development of Sri Lankan natural vein graphite to the anode of Li-ion rechargeable batteries, through purification and surface modification have been investigated recently. Furthermore, natural graphite has to be structurally modified by expanding interlayer distance to facilitate the intercalation of larger Na^+ ions for the application in rechargeable Sodium Ion Batteries (SIB) (Wei, 2011). The present study investigated the possibility of expanding the interlayer distance of Sri Lankan natural vein graphite for accommodating Na-ion intercalation by converting into Graphite Oxide (GO).

Materials and methods

Purified samples from all four structural varieties of Sri Lankan vein graphite, were used in this study. Raw graphite samples were oxidized to Graphite Oxide (GO) by using improved hummers method (Madusanka Y.N., Amareweera T.H.N.G.,Wijayasinghe H.W.M.A.C., 2013). In this method 96% H_2SO_4 (Sigma-Aldrich) and 85% H_3PO_4 (Sigma-Aldrich) were added to purified vein graphite. Then $KMnO_4$ (Belgolabo) was added little by little to the mixture with in two hours and stirred. Sample was allowed to cool until room temperature. Solution was poured into 30% H_2O_2 in an ice bath and the sample was vacuum filtered using Fisher brand filter papers using distilled water.

The d.c. electrical conductivity of raw graphite and prepared GO samples were measured using the standard four probe method. Fourier Transform Infrared (FTIR) spectra of raw graphite and GO samples were employed to study the structural modification. Further the X-ray diffractometry was used to confirm the formation of GO.For the Na-ion intercalation study, the modified graphite

oxide was tape casted by the doctor blade method to fabricate electrodes. GO was the active material, carbon black was selected as the conductive additive and the binder was polyvinylidene fluoride (PVDF). All the materials were weighed using a chemical balance and placed in a small beaker. Then excessive amount of acetone and dimethylformamide (1:1 ratio) were added to the beaker, covered with an aluminum foil and stirred for 12 hours. Mixture was poured on to a copper foil pasted on a glass to form a very thin layer. It was allowed to dry. The electrodes were fabricated by cutting the copper foil to required shape. A half-cell was assembled using the fabricated GO anode with a gel electrolyte and sodium metal as the reference electrode. Assembling and testing of the cell was conducted inside a N_2 filled glove box. Discharging current of the half-cell under 0.5 kΩ load over time was measured and it was recorded using a computer interfaced program.

Results and Discussion

As shown in Figure 1, the FTIR spectra confirmed the presence of functional groups of alcohols, carboxylic, carbonyls and phenol. These functional groups are present in GO, which are not in raw graphite, indicate a successful conversion of graphite into GO. FTIR spectra also confirm the presence of non-oxidized carbon rings in the GO.
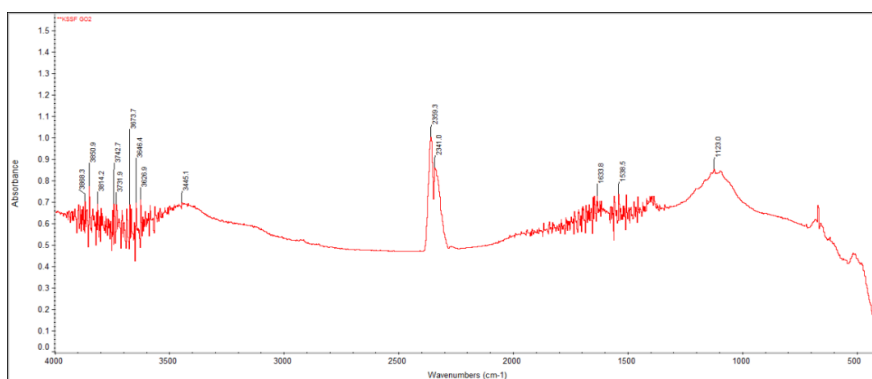

Figure 1: FTIR spectrum of GO prepared from SSF graphite

Degrees 2-theta
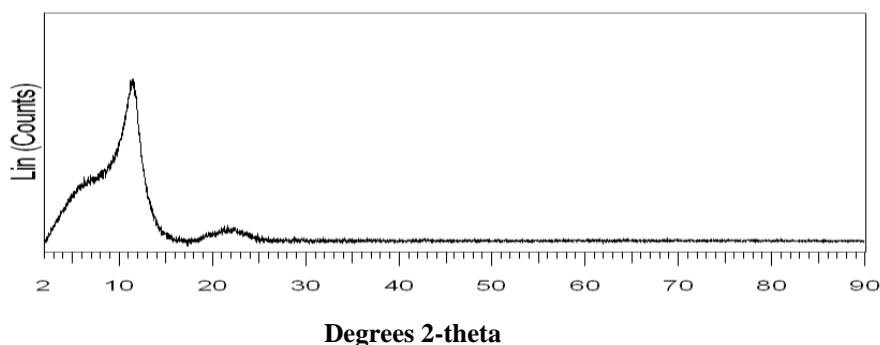
Figure 2: XRD spectrum of GO synthesized from CSF graphite

The XRD spectrum of graphite oxide which is shown in Figure.2 has two peaks at 22.50 and 11.00 degrees and these peaks are slightly shifted to the left side when compare to the XRD pattern of graphite (Madusanka Y.N., Amareweera T.H.N.G.,Wijayasinghe H.W.M.A.C., 2013).Graphite Oxide is showing a prominent broad peak at 11.00 degrees and analyzing these peaks can easily identify the oxidation and hydration level of the GO sample. This is a direct indication for the oxidation of graphite.

Conversion of natural graphite into GO has drastically decreased the electrical conductivity indicating the formation of low conducting oxide materials. Out of the four GO samples prepared in this study, the SSF shows the highest electrical conductivity of 1.6×10^{-5} S cm^{-1} while the CSF has the lowest conductivity of 3.2×10^{-6} S cm^{-1} at 25 ^{0}C.Figure 3 shows the discharge characteristics of the cell with configuration GO(developed) /GPE/ Na metal at room temperature for constant load of 0.5 kΩ. The open circuit voltage (O.C.V.) of the cell was about 2.9 V and the initial voltage drop was concluded due to the formation of electrode - electrolyte interface.

The discharge current-time characteristics of the cell exhibits a low stable current value due to the cell fabrication failures such as oxidation of the sodium metal caused by atmospheric exposure.
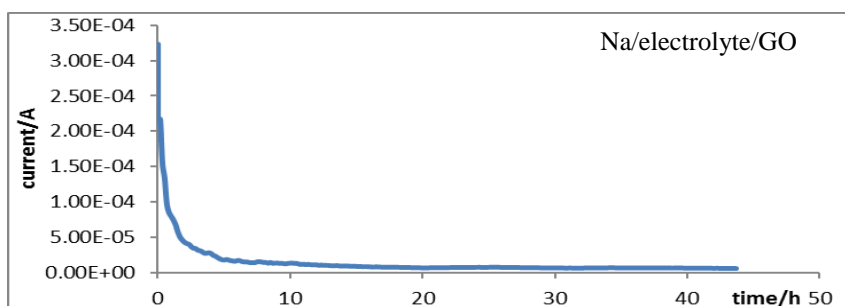
Figure 3: Current vs time curve of half-cell

Conclusions

This study revealed the possibility of structural modification of all four varieties of Sri Lankan natural vein graphite by oxidizing graphite into GO using improved Hummer's method. FTIR spectra gave the evidence for successful oxidation of graphite into GO and the XRD phase analysis further confirmed the transformation. In cell testing of the Na/electrolyte/GO half-cell gave a significant O.C.V. of 2.9 V. It is a clear evidence for the possibility of intercalating relatively larger but more abundant and low cost ions like Na$^+$ ions to GO. Altogether, this study indicates the possibility of structurally modification of Sri Lankan natural vein graphite for the anode application of Na-ion battery.

Acknowledgement

The technical staff of Institute of Fundamental Studies for the technical support during this study

References

Balasooriya N.W.B, Bandaranayeke S.K. (2010). <u>Vein Graphite from The Bogala And Kahatagaha–Kolongaha Mines.</u>

Wei. (2011). Ph.D Thesis, <u>Graphite Oxide: Structure, Reduction and Applications,</u>Rice University.

Madusanka Y.N., Amareweera T.H.N.G.,Wijayasinghe H.W.M.A.C. (2013). <u>Synthesis of Graphite Oxide from Kahatagaha Vein Graphite using a Localized Improved Hummers Method</u>. Uwa Wellassa University.

Reinforcement of natural rubber using silica and zeolite mixed fillers

L. W. S. Dilhan, R. M. M. D. Rathnayake, and C.K. Jayasuriya

Faculty of Science, University of Kelaniya

Introduction

Among the main ingredients added in the compounding process of Natural Rubber (NR), fillers play a major role. The purpose of adding fillers into the rubber matrix is 2-fold: to reduce the production cost or to give reinforcement. (Blackley, 1997). A reinforcing filler would increase the mechanical properties such as tensile strength, elongation at break, and tear resistance of the rubber vulcanizate. Increasing the area of contact between rubber matrix and filler particles, and increasing the degree of bonding between the two phases seem to be the most important factors in providing the strong reinforcement effect (Treloar, 2005). The current research is focused on a combination of two fillers, namely silica and zeolite, to provide a reinforcing effect on NR. Silica is in general widely used for reinforcement of NR. On the other hand, zeolites were considered due to their unique porous structure which would enhance the area of contact between the phases.

Methodology

Materials

Double Centrifuged Natural Rubber Latex (DCL) with 60% dry rubber content (stabilized with ammonia) provided by Dipped Product Industries in Sri Lanka was used in the preparation of the samples. Mineral samples, Silica and Zeolite were purchased from Glorchem, Colombo. The rubber additives, namely, zinc oxide, sulphur, antioxidant, dispersing agent, Zincmercaptobenzothiozole (ZMBT), Zincdiethyldithiocarbamate (ZDDC), Diphenylguanidine (DPG), etc) were of commercial grades.

Procedure

The samples were prepared using NR latex compound formulation used for glove manufacture. The mineral samples were ground using "TEMA mill" and were sieved to get the particle sizes in the range of (45 – 60) μm. A stabilized natural rubber was obtained by adding potassium laurate (20%) and KOH (10%, 2.50 g) to natural rubber latex (60%, 167 mL). ZnO (1.00 g), Zincdiethyldithiocarbamate (0.20 g), Zincmercaptobenzothiozole (1.00 g), Diphenylguanidine (1.20 g), antioxidant (1.50 g), dispersing agent (0.20 g) and Sulphur (1.40 g) were ground together using a mortar and a pestle. The ground mixture was dissolved in distilled water (8.30 mL) using a magnetic stirrer to obtain the dispersion. The stabilized NR solution and the dispersion were mixed together and distilled water was added to dilute the total dry rubber content of the solution up to 40%. This sample was labelled as "NR" and was used as the control sample.

The amount of mineral needed to make up 1%, 2%, 3%, 4% and 5% of the final weight of the sample was calculated and added to the dispersion. In this research, two series of samples were prepared: first series was prepared by adding silica as the mineral and was labeled "Sil" and the

second series was prepared by adding a 1:1 mixture of Silica and Zeolite as the mineral and was labeled "Mix". Calculated amounts of sieved minerals were added to both series. The solutions (NR, Sil and Mix) were then filtered and poured into small glass tanks, covered and left overnight to dry. The samples were then cured for 3.5 min at 120 °C using the hot box oven (Gallencamp). The entire procedure was triplicated.

The mechanical property analysis was based on tensile and tear strength. The samples with optimum mineral percentages showing the best tensile and tear properties were subjected to the structure determination by Fourier Transformed Infrared (FTIR) analysis and thermal properties by thermogravimetric analysis (TGA).

Results and Discussion

The variation of tensile strength as the type and the amount of mineral filler in NR samples are varied is given in Figure 01.
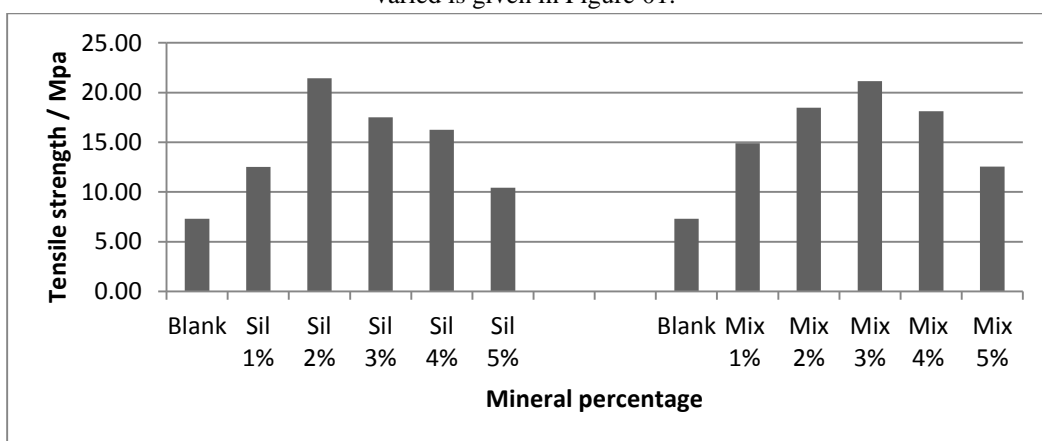
Figure 01. The variation of tensile Strength with varying the type and amount of mineral filler

According to the results, the tensile strength is increased with increasing mineral percentage up to a certain level in both silica and mixed fillers and further increase of mineral percentage has caused the tensile strength to decrease. The maximum tensile strength value for silica loading samples (Sil) was observed at 2% and the relevant value for mixed mineral loading samples (Mix) was observed at 3%. Both type of samples had shown a nearly 200% increment in tensile strength at its optimum load of mineral in the sample, compared to the Blank sample. Similar observations were made for tear strength analysis as well. Enhanced tensile and tear properties of NR at low loads of filler can be explained by polymer–filler interactions and filler–filler interactions within the polymer. However, the expected reinforcement in the filled samples with mixed minerals was not very promising. Porous structure of zeolites combined with reinforcing properties of silica, was expected to give a marked increase in mechanical properties. The ratio of silica and zeolite used, 1:1, may not have produced sufficient polymer-filler interactions. However, when the filler content is higher than 4%, the filler would tend to agglomerate leading to the observed reduction of tensile strength.

The Fourier-Transformed Infra-Red (FTIR) spectra confirmed the incorporation of fillers showing peaks at corresponding frequencies and cleavage of bonding in the filled samples due to the insertion of silica and zeolite into the NR matrix (White, *et al*, 2001).

TGA results of selected 5 samples are given in Table 01. The temperature at which 3% sample weight loss occurs ($T_{3\%}$) is considered as the degradation onset temperature. The temperature at which the highest weight loss rate occurs is set as the degradation temperature (T_{max}).

Sample	Degradation onset Temperature / °C ($T_{3\%}$)	Degradation Temperature / °C (T_{max})	Percentage Weight loss at 200 °C
Blank	180	200	3.0
2% Sil	210	225	2.8
3% Sil	215	223	2.0
2% Mix	210	226	2.7
3% Mix	225	235	2.1

Conclusions

Both tensile and tear properties of NR are improved at low loads of filler. However, when the filler content is higher than 4%, the tensile and tear properties are reduced. The expected reinforcement in the filled samples with mixed minerals of silica and zeolites was not very promising. The ratio of silica and zeolite used, 1:1, may not have produced sufficient polymer-filler interactions. Further research must be carried out by varying the ratio of silica and zeolites to determine the optimum ratio which would provide the greatest reinforcement. However, the thermal properties of all the filled samples are significantly increased.

Acknowledgement

References

Blackley, D.C. (1997). *Polymer Lattices, Science and Technology, volume 1: Fundamental Principles. 2nd ed. Chapman & Hall. New York*.

Treloar, L. R. G. (2005) *The physics of rubber elasticity. Oxford University Press, U.K.*

White, J,R., Naskar, K. and De, S.K. (2001) *Rubber technologist's handbook. Rapra Technology Limited, Polestar Scientifica, U.K*

Effect of Low pH of Groundwater in Rathupaswala Area, Sri Lanka: A Case Study

W.A.V Premalal

Department of Science and Technology, Uva Wellassa University

and

D.T Jayewardene

Department of Forestry and Environment, Sri Jayawaradanapura University

Introduction

Groundwater occurs in different type of aquifers under various geological conditions. Sri Lanka has a centrifugal pattern of groundwater movements which effectively controlled by the geomorphological characteristics of the terrain. This study is focus to Rathupaswala area in the western province which was highly controversial during the past due to low pH groundwater. The area is covered within Attanagalla basin which has dendritic drainage pattern. The lateritic aquifer system is common in the study area consisting of hard and soft laterite soil which is usually considered as a very good filter media for groundwater. (Wijesekara, 2011).

Objectives

The research is mainly aim to identify the mobility of selected trace elements (Fe, Mn, Cr, Zn, Cs, Sr, Rb, and Li) into the groundwater under prevailing low pH condition and to identify the water type of the area using selected major cations (Na^+, K^+, Ca^{2+}, Mg^{2+}) and anions (SO_4^{2-}, Cl^-, CO_3^{2-} and HCO_3^-) to investigate possible geochemical processes that can be take place under natural low pH.

Methodology

Thirty (30) selected groundwater samples were collected from the shallow and deep wells and in-situ measurements of pH, Oxidation Reduction Potential (ORP), conductivity and turbidity were done just after collecting of the samples. Selected cations were analyzed using Atomic Absorption Spectrometer (AAS). In addition, sulfate analysis were done using nephelometer. Conversely element chloride, carbonate and bicarbonate were analyzed using respective titration methods. Multivariate statistical analyses were used to determine the correlations between the elements and the physiochemical properties by means of minitab14 software.

Results and Discussion

Average values of cations and anions and the physiochemical parameters indicate that lower effects on groundwater in the area. Results further show that strong positive relationship between Mg-Mn, Li-Rb and Na-K. Significant strong positive relationship between K-Mn. Positive relationships between Na-Mn and Na-Mg. Correlations between those elements may reflect the weathering evidences of ferromagnesian minerals available in the basement.

However, pH show negative relationship with Na, K, and Mg. This may reflect lack of sulfide bearing minerals with ferromagnesian minerals which usually help to create acidic pH for soil and water. This concluded that the lower pH is not due to mineral weathering in the basement in the area. Other elements such as Ca, Mn, Fe, Cu, Zn, Li, Sr, Cs, Rb, chloride, sulphate and bicarbonate show very poor trends with pH. This further reflect possible evidences for lower impacts of mineral weathering on low pH groundwater. Conductivity shows positive relationships with Na, K, Mg and Mn which reflect salinity of groundwater is controlled from those elements and they considered as basic cations which help to buffer the lower pH. Only calcium shows stronger positive relationship with turbidity may be due to calcium carbonate sources. In general, it can be concluded that lower pH groundwater in the area is not directly associate with mineral weathering phases in the basement rocks.

Piper classification is used to determine the available water type. The classification indicate that the Na-bicarbonate water (51.6%) as the major water type present in the area and Ca-Na-bicarbonate (35.5%) type water is also dominantly present. In addition, few samples from the area reflect high concentration of Mn.
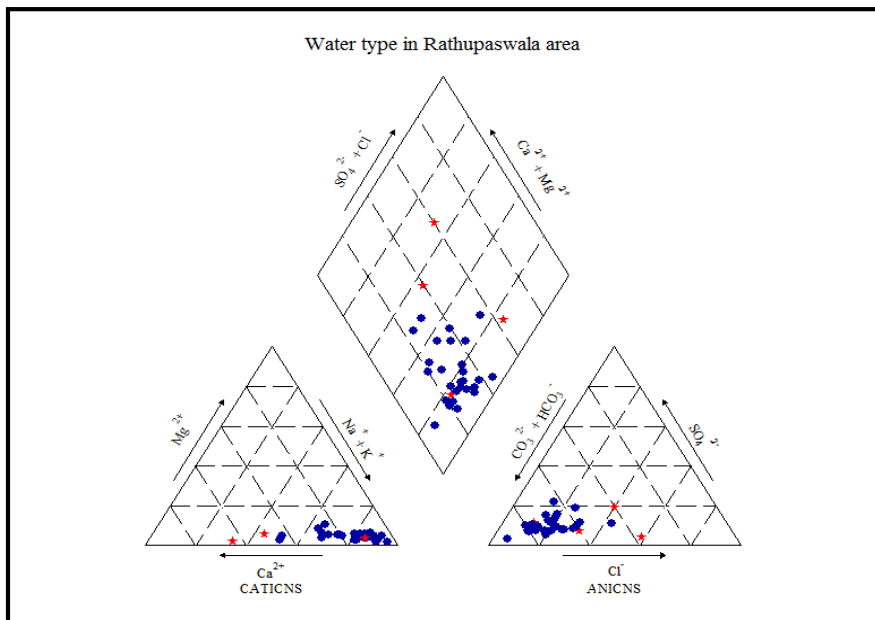
Figure 3: Piper plot diagram-Water type in Rathupaswala area

Conclusion

The majority water type in the studied area is Na-Bicarbonate. Cu, Zn and Fe can be in the soil with mineral bearing rocks and added as an individual source. It is also shows that there is no artificial impact for the groundwater. The other elements Na, K, Mn, Ca, Mg, Li and Rb shows relationships due to the low pH values. The average pH not harmful and shows entire water field not under redox conditions. Groundwater samples in studied area do not exceed the SLS standards for drinking water parameters. Hence the groundwater not hazardous for the human consumption.

References

Panabokke, C. (2007). Groundwater Conditions in Sri Lanka. National Science Foundation of Sri Lanka.

Wijesekara, R. (2011). Proceeding of The Workshop On Challenges in Groundwater Management in Sri Lanka. Retrieved from http://www.wrb.gov.lk/web/images/stories/downloads/Scientific_Reports/proceeding_07_april_11.pdf

Hydrological assessment of flow in Uma Oya, Sri Lanka

U. S. Rathnayake

Department of Civil Engineering, Faculty of Engineering, Sri Lanka Institute of Information Technology, New Kandy Road, Malabe, Sri Lanka

Introduction

A current meter is usually used in river flow measurements. However, if someone is interested in obtaining the temporal variation of a particular river, it may not be the easiest method in the world to use a current meter (i.e. daily) to measure the flow rate. In such events, the stage measurements can be taken and then, they can be converted to the flow rates (USGS, 2014). One can use the stage-discharge relationship to find the corresponding flow rate (Mortuza *et al.*, 2011; Raj and Azeez, 2009; Gupta and Chakrapani, 2005).

However, this method still requires some flow measurements to produce the stage-discharge relationship. Therefore, a current meter should be there to measure the velocities and then, to calculate the flow rates. In case of absence of a current meter, one has to think another way of obtaining the flow hydrograph. This paper presents a simple approach in obtaining the flow hydrograph for a river in Sri Lanka: Uma Oya. Uma Oya catchment is being modeled and this study shows some preliminary results. The detailed flow hydrograph for Uma Oya for a longer period is being developed for the frequency analysis. The developed flow hydrograph is being used to model the Uma Oya catchment in Sri Lanka.

Uma Oya catchment

The catchment of Uma Oya upper watershed was found to be around 750 km^2 (Dam safety and Water resources planning project component report, 2010; Dissanayake *et al.,* 2010). However, a detailed catchment analysis is being carried out and the catchment areas will be listed in the future publications. Since it is in upcountry of Sri Lanka, steep slopes are quite frequent along the river. It has even reached about 1900 m MSL (Dissanayake *et al.,* 2010). The catchment is basically a green catchment. Natural forests, tea estates, paddy fields and potato farming lands are commonly seen in the catchment (Dam safety and Water resources planning project component report, 2010; Dissanayake *et al.,* 2010). Natural forests cover the highest elevations. Then, tea estates, potato farms and other vegetable and paddy fields cover the lower elevations.

Uma Oya is one of the main tributaries in Mahaweli River. It flows into the Rantambe reservoir (refer Figure 4). The upper catchment is hardly conserved from soil erosion; therefore, a significant amount of sediment flows into the reservoir. Sediment deposition can be visually evidenced in the Rantembe reservoir. Therefore, the reservoir faces the reduction of its water holding capacity and then, the reduction of electric generation capacity. In addition, Uma Oya catchment is one of the rainy catchments in the country. Therefore, it has a wealthy sediment flow.

Rainfall patterns in Sri Lanka

Sri Lanka is a country blessed with water resources. Unlike most of the other countries in the region, it has rain throughout the year. It has two monsoons and two inter-monsoon rainy seasons. The diagram given in Figure 01 shows the rainfall patterns in Sri Lanka throughout the year. Temporally, Sri Lanka has no dry seasons; however, spatially, there are some dry periods to some parts of the country. For example, some locations in Jaffna, Batticaloa and Mannar get a little rain during the south-west monsoon season (May to September).

Mar	Apr	May	Jun	Jul	Aug	Sep	Oct	Nov	Dec	Jan	Feb
1st Inter-monsoon season		South-west monsoon season					2nd Inter-monsoon season		North-east monsoon season		

Figure 01: Rainfall patterns in Sri Lanka

Since this paper targets the catchments of Uma Oya, the discussion of rainfall is limited to a particular one season; north-east monsoon season. North-east monsoon season dominates most of the north and eastern part of the Sri Lanka including Uma Oya catchment. The Figure 02 gives the spatial variation of rainfall during the north-east monsoon season. Northern and eastern slopes of the hill country and the eastern slopes of the Knuckles / Rangala ranges experience the highest rainfall from this monsoon (Meteorology department, Sri Lanka). The maximum-recorded rainfall was to Kobonella estate whereas the minimum was to Chilaw. According to the Figure 02, it can be clearly seen that Uma Oya catchment gets a significant amount rainfall during the months of December to February (red squared section).
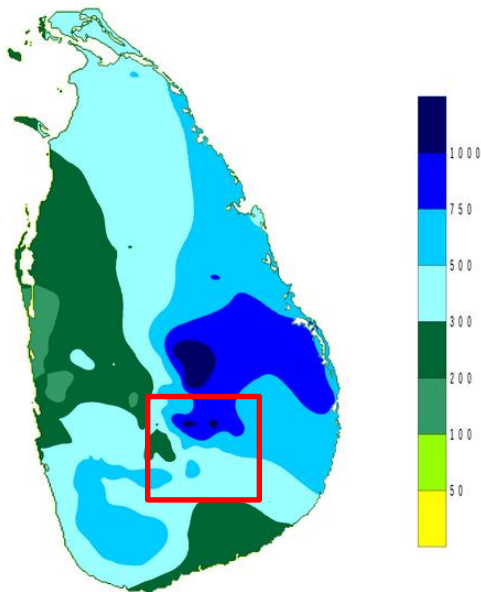
Figure 02: Rainfall variation across Sri Lanka due to north – east monsoon (Department of Meteorology, Sri Lanka)

Flow hydrograph from Uma Oya to Rantembe reservoir

A schematic diagram of a reservoir is presented in Figure 03. I_t and O_t are the inflows and outflows from the reservoir, respectively.
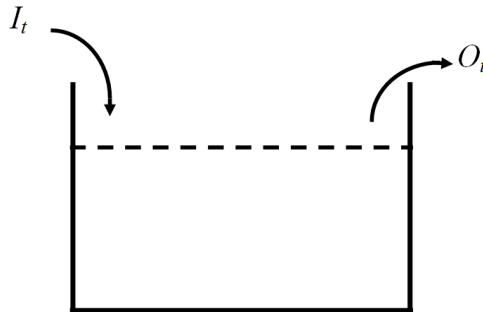
Figure 03: Schematic diagram of a reservoir

Referring Figure 03, a simple continuity equation for reservoir routing can be drafted (Equation 01). This equation can be used to calculate the temporal variation of any unknown from inflow, outflow or capacity while the other two variables are given.

$$\frac{S_{t2} + S_{t1}}{\Delta t} = \left(\frac{I_{t1} + I_{t2}}{2} \right) - \left(\frac{O_{t1} + O_{t2}}{2} \right); \quad \Delta t = t2 - t1 \tag{01}$$

where S_{ti}, I_{ti} and O_{ti} are the capacity of the reservoir, inflow to the reservoir and outflow from the reservoir at time ti, *respectively.* Δt is the time step for the temporal variation.

Rantembe reservoir has two main and one minor inflows as shown in the Figure 04 (I_R, I_U & I_M). I_R represents the outflow from the Randenigala reservoir. This outflow can be either the flow from Randenigala hydropower station or the summation of hydropower station and any spilling. I_U is the flow from Uma Oya and I_M stands for the inflow from a small creek called Maha Oya. However, compared to I_R and I_U, I_M is much lower (as it is a small creek).
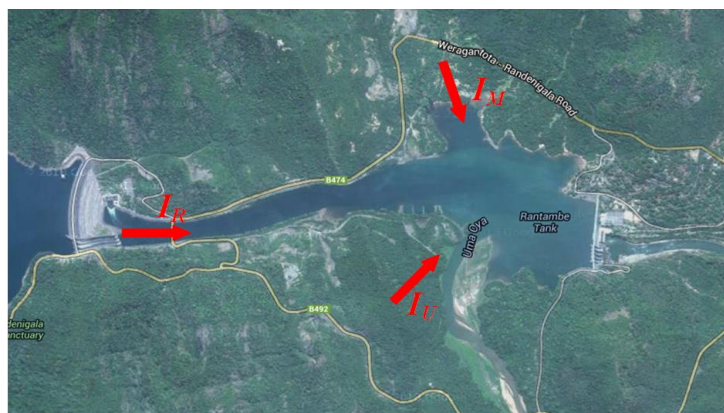
Figure 04: Flow characteristics for Rantembe reservoir (Photo – Google maps)

Given that the temporal variations of storage in Rantambe reservoir and the outflows from Rantambe reservoir (both for hydropower generation and spilling flows) are availalbe, one can find the temporal variation of the inflow to the Rantambe reservoir from Uma Oya. Therefore, the flow hydrograph of the Uma Oya at Rantambe reservoir is available.

The height VS volume curve for Rantembe reservoir is avialble. The reservoir specific curve is given in the Figure 05. Assuming that the curve hasn't been deviated its original from the sediment inflow, it can be used to find the volume of the water stored in the reservoir by measuring (observing) the water height in the reservoir. Therefore, this realtionship can be effectively used to calculate the S_{t1} and S_{t2} terms in Equation 01.
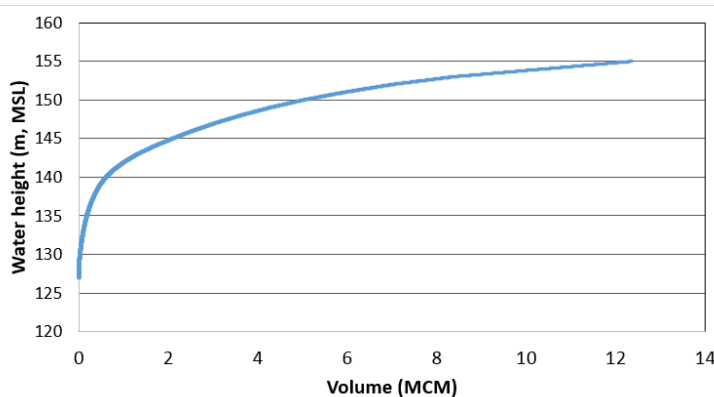
Figure 05: Rantembe reservoir height VS volume relationship

The outflow (O_{t1} and O_{t2}) from the reservoir can be found from the data available on spills and electricity generation. Therefore, the temporal variation of inflows can be calculated.

Result and Discussion

Figure 06 shows the flow hydrograph from Uma Oya to Rantambe reservoir during several days in the month of December in year 2004. This figure clearly shows the diuranal pattern of the flow. Daily average flow is found to be 180.7 m^3/s. However, the maximum flow rate during this period was 605.5 m^3/s while the minimum was 8.6 m^3/s. It can be clearly seen herein that the peak flows are usually during the night or late night time of the day.
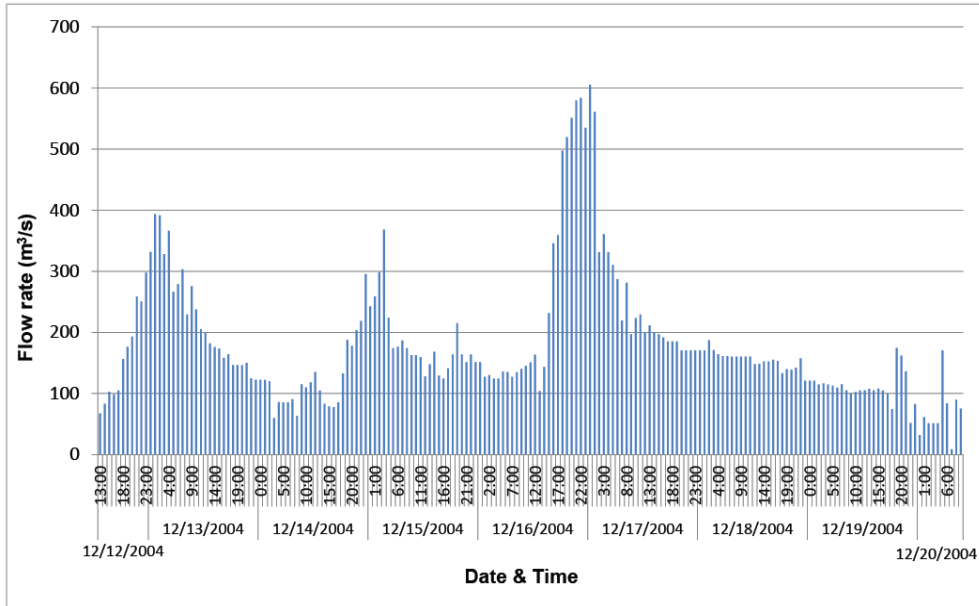
Figure 06: Flow hydrograph for Uma oya

However, the developed hydrograph is for a limited period. Therefore, this hydrograph can not be used for a frequency analysis. However, the research is being carried out to develop a detailed hydrograph for Uma Oya.

Conclusions

Uma Oya catchment is being modeled. This paper shows the preliminary results of obtaining the flow hydrograph of Uma Oya. The flow hydrograph for Uma Oya at Rantembe reservoir is developed; however, the completed flow hydrograph is being developed for the hydrological analysis of the Uma Oya catchment.

Acknowledgements

Author would like to extend his gratitude to Mahaweli Authority of Headworks, Rantembe, Sri Lanka for providing the required data for this analysis.

References

Climate in Sri Lanka, Department of Meteorology, Sri Lanka http://www.meteo.gov.lk/index.php?option=com_content&view=article&id=106&Itemid=81& updated on 02 – May – 2012, accessed on 10 – Nov – 2014.

Dam safety and Water resources planning project component 3 – Multi-sector water resources planning (2010). *Report by SMEC International Pty Ltd. in association with DHI Water and Environment (Denmark) Ocyana Consultants.*

Dissanayke, C.K., Mahawatte, P., Abenayake, K. and Weerasekera, T.S.B. (2010). Use of Caesium-137 technique for the assessment of soil erosion in two selected sites in Uma Oya catchment in Sri Lanka. *19th World Congress of Soil Science, Soil Solutions for a Changing World, 1st – 6th August 2010, Brisbane, Australia, pp. 165-168.*

Gupta, H. and Chakrapani, G.J. (2005). Temporal and spatial variations in water flow and sediment load in Narmada River basin, India: natural and man-made factors. *Environmental Geology*, **48**, pp. 579-589.

Mortuza, M.R., Rashid, U.S., Rajib, M.A. and Rahman, M.M. (2011). Temporal variation characteristics of flow and water levels in the Old Brahmaputra River. *International Symposium on Water Resource and Environmental Protection (ISWREP), 20th – 22nd May 2011, Xi'an, China,* pp. 1132-1135.

Raj, N. and Azeez, P.A. (2009). Spatial and temporal variation in surface water chemistry of a tropical river, the river Bharathapuzha, India. *Current Science*, **96(2)**, pp. 245-251.

USGS (2014) - How stream flow is measured? http://water.usgs.gov/edu/measureflow.htm/ by U.S. Department of Interior and U.S. Department of Geological Survey, updated on 17 – March – 2014, accessed on 18 – Dec – 2014.

Investigation of Trihalomethanes formation in Greater Kandy Water Treatment Plant and its distribution

M. G. N. Perera

Faculty of Science and Technology, Uva Wellassa University of Sri Lanka

and

Dr. S. K. Weragoda

National Water Supply and Drainage Board, Kandy, Sri Lanka

Introduction

No doubt that chlorination has been successfully used for the control of water borne infections diseases for more than a century. Halogenated trihalomethanes (THMs) and haloacetic acids (HAAs) are two major classes of disinfection byproducts (DBPs) commonly found in waters disinfected with chlorine (Rook, 1974). The formation of the Trihalomethanes (THMs) was investigated in Greater Kandy Water Treatment Plant (GKWTP) and distribution system which serve drinking water to Kandy region, located in the middle province of Sri Lanka. Water samples were taken from storage tank of GKWTP of the National Water Supply and Drainage Board (NWS & DB), covering selected water quality and operational parameters that have direct influence on THM formation. In addition THM formation at the distribution extremities were also studied.

Methodology

Water samples were taken from storage tanks of GKWTP after the chlorination of initial dosage of 2 ppm chlorine. Water samples of 32 taken from selected distributed within six Divisional Secretariat Divisions for the analysis. Primary Trihalomethanes were analyzed using Gas Chromatography – ECD (Kuivinen, 1999). Formation of Trihalomethanes were analyzed in storage tanks for 64 hours by doubling time and level of Trihalomethanes in distribution system. Apart from THMs, pH, temperature, turbidity, were analyzed in raw water and treated water collected at sampling points by pH meter, thermometer and turbidity meter respectively. Treated water was also tested for free chlorine level and total chlorine level to observe impact on THM formation by those parameters by colorimeter.

Result and Discussion

Measured THMs and other parameters for storage tanks in GKWTP summarized in Table 1 and indicate in figure 1. This indicate that the trihalomethanes increase with the time in storage tanks. Initially mean TTHMs was 17.09 µg/L when the initial dose of chlorine of 1.85 mg/L. When doubling the reaction time formation of THMs were increased and finally it became 40.72 µg/L when reaction time become 64 hours. Table 1 indicates that the free chlorine and total chlorine decaying with time. Temperature is constant for the whole analysis as 25. C, as it highly depend

on temperature. Concentrations of $CHCl_3$, $CHCl_2Br$ and TTHM of sampling locations indicate in Table 2 in 32 sampling points. Table 2 summaries descriptive statistics for individual and total THMs (TTHMs) with free chlorine in the water samples of distribution system. Highly variable range of TTHMs concentrations were found (11.275 to 22.976 µg/L) in distribution system. Chloroform ($CHCl_3$) concentrations contribute a significant portion to the TTHMs (76%) while Bromodichloromethane ($CHCl_2Br$) contribute 24%.

Regression model for GKWTP. The regression equation is:

TTHM (µg/L) = 19.5 + 0.00580 Time (min)   R-Square (adjusted) value = 95.9%; $p < 0.05$

Conclusions

When considering storage tanks conclude that the formation of trihalomethanes depend on reaction time and free chlorine while temperature, pH, turbidity remains constant. CHCl3, CHCl2Br and TTHMs levels at all locations were found lower than the guideline values regulated in WHO and USEPA which is lower than 25 µg/L. Due to the free chlorine ranges to 0.2 to 0.7 mg/L in distribution system, conclude that residual chlorine exceeding its standard value of 0.2 mg/L for drinking water. Variation of trihalomethanes and free chlorine values of storage tanks and distribution system, assume that chlorine reactions take place and evaporation of free chlorine during analysis. Other two compounds of trihalomethanes such as Dibromochloromethane (CHClBr2), and Bromoform (CHBr3) could not be detected in GKWTP.

Table 1:- Mean values of THM formation in drinking water (GKWTP)

Time (min)	CHCl3 µg/L	CHCl2Br µg/L	TTHM µg/L	pH	Temp .C	Turbidity NTU	Free chlorine mg/L	Total Chlorine mg/L
0	13.8797	3.20567	17.0853	7.35	25	0.13	1.65000	1.84667
15	15.0257	3.66033	18.6860	7.35	25	0.13	1.64667	1.83000
30	16.2490	3.64800	19.8970	7.35	25	0.13	1.57667	1.99333
60	16.0750	3.76000	19.8350	7.35	25	0.13	1.59667	1.72667
120	16.2653	3.86500	20.1303	7.35	25	0.13	1.58333	1.72333
240	17.0267	4.30367	21.3303	7.35	25	0.13	1.51667	1.68333
480	18.3473	4.22367	22.5710	7.35	25	0.13	1.44000	1.59000
960	22.8537	5.27133	28.1250	7.35	25	0.13	1.21000	1.36000
1920	25.5840	5.50600	31.0900	7.35	25	0.13	1.20667	1.34000
3840	34.4920	6.22700	40.7190	7.35	25	0.13	0.85667	1.00333

Table 2:- Minimum (Min), Maximum (Max), Mean, Median and Standard Deviation (SD) levels of THM formation in drinking water (distribution)

	CHCl3 (µg/L)	CHCl2Br (µg/L)	TTHM (µg/L)	Free chlorine (mg/L)
Min	6.706	2.481	11.275	0.200
Max	19.481	6.168	22.976	0.700
Mean	13.885	4.274	18.159	0.560
Median	14.185	4.243	18.058	0.550
SD	3.038	1.060	2.871	0.107
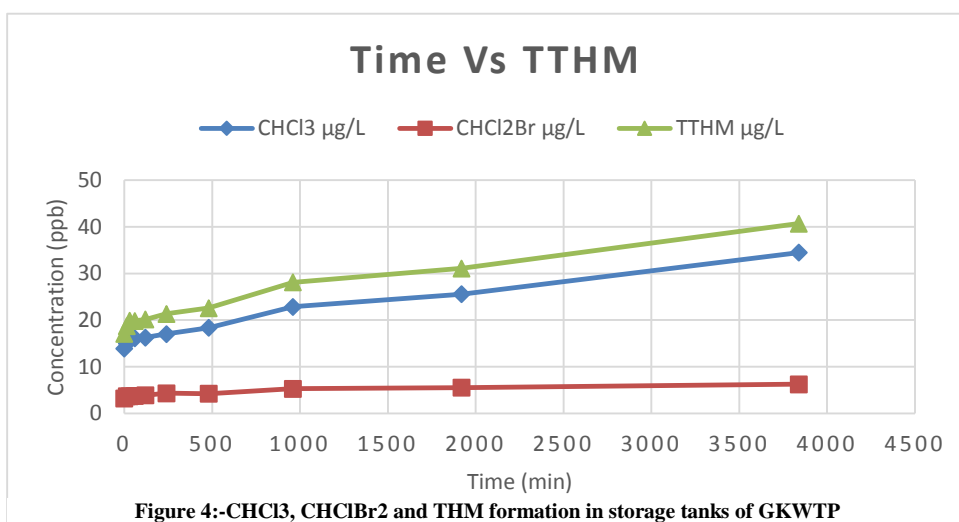
Figure 4:-CHCl3, CHClBr2 and THM formation in storage tanks of GKWTP

Acknowledgement

References

J. Kuivinen, H. Johnsson. (1999). Determination Of Trihalomethanes and Some Chlorinated Solvents In Drinking Water By Headspace Technique With Capillary Column Gas-Chromatography, Wat. Res. Vol. 33, No. 5, pp. 1201±1208, 1999.

Rook, J.J. 1974, Formation of haloforms during chlorination of natural waters, Water Treatment Examination, vol, 23, pp. 234-243.

Water pollution study in Nalanada Lake to improve the Water quality of Naula Water Treatment Plant

T.N.T.K. Nawarathna

Uva Wellassa University, Badulla, Sri Lanka

and

M. Makehelwala

Greater Kandy Water Treatment Plant, Katugastota, Sri Lanka

Introduction

Water is the largest natural resources of Sri Lanka although only a relatively low percentage of total population is getting safe and clean water for daily use. Water is using for Drinking, bathing, washing, and cleaning. Beside it is used for agriculture, industrial, hydropower generation.

The Nalanda reservoir located in Naula, Matale district is the main water source of Naula Water Treatment Plant of National Water supply and Drainage Board (NWSDB). On the other hand NWSDB faces a big problem in the dry season because pumping water had a less amount of Dissolved Oxygen (DO) and occurring black color in pumping water. The dissolved oxygen (DO) concentration is a primary measurement of a stream's healthiness. The dissolved oxygen concentration responds to the biochemical oxygen demand (BOD) load. Investigators have continuously studied the dissolved oxygen uptake characteristics in stream water in relation to different sinks and sources in order to develop mathematical models describing the DO consumption.

In this reservoir percent high amount of Algae due to high nutrients content such as nitrate and phosphorous and change that algae type seasonally. One of the objectives of this research study is that Nitrate and Phosphorus variation in reservoir. And Main Objective was identification of the Dissolved Oxygen (DO) Variation in Nalanda reservoir.

Methodology

In this study six sampling location points were selected and studied the variation of nitrate, phosphorous and DO of these sampling points for four weeks of time. These data were collected in rainy and dry season. Samples were collected from the different distances from the intake of Naula Water Supply System. Totally 24 samples were collected from the upstream of the reservoir. Basically, the selected pollution points are surrounding point of the reservoir. Samples were taken from different morphological units of the reservoir. DO was analyzed at the sample collected points and COD and BOD also analyzed using the Standard laboratory procedures. Finally DO concentration variation was analyzed by using mathematical model called Streeter-phelps.

Results and discussion

Eutrophication of water body is occurred under high nutrients. The nutrients such as nitrate and phosphate distribution within selected pollution points in Nalanda reservoir is shown in figure 1. The recommended phosphate level for maintaining healthy water to minimize algae growth is 0.1 mg/L and nitrate level is 10 mg/L (USEPA). The results shown below indicated that the nitrate level was within required limit and phosphate level was exceeded limit. Therefore, phosphate consuming algae species can occur in Nalanda reservoir during this period.
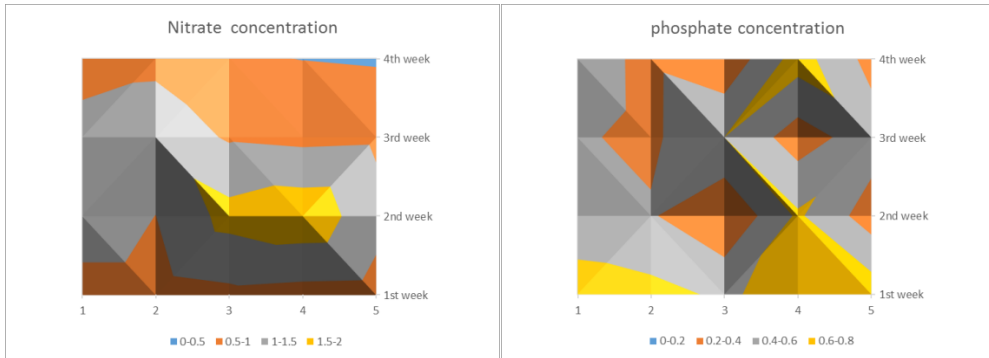
Figure 1: Nitrate and phosphate concentration variation within selected pollution points in Nalanda Reservoir

Here, we used the mathematical equation called Streeter-Phelps equation to identify oxygen consumption by aerobic BOD degradation and DO recovery by dissolution from water surface. The data obtained from DO sag curve is summarized in Table 1. The position where the lowest DO appeared was around 14 – 18 km. If dissolved oxygen levels in water drops below 5.0 mg/ the aquatic life is under stress. According to our data, the lowest DO appeared around 5.6 – 7.5 ppm. Therefore it is not under stress conditions. A high DO level in a water supply gives better taste for drinking water. However, high DO levels speed up corrosion in water pipes.
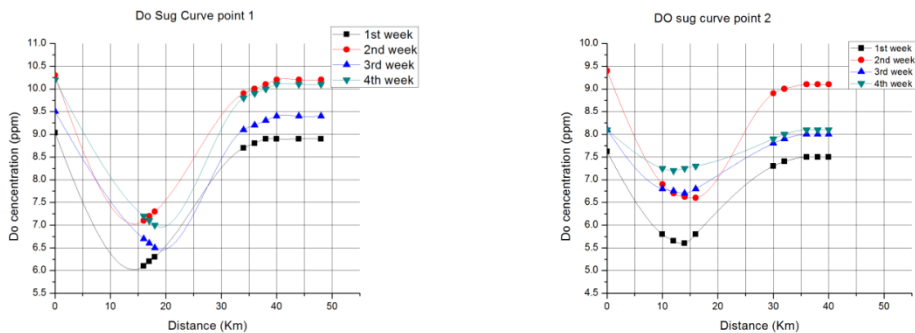
Figure2: DO sag curves in Sample collected Point 01 and 02
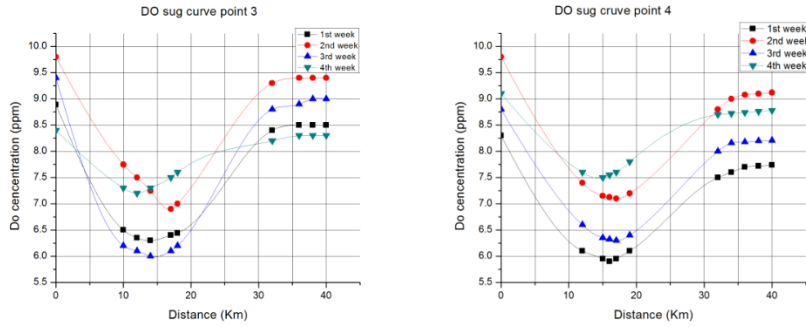
Figure3: DO sag curves in Sample collected Point 03 and 04

point	week	Initial DO/ppm	Critical DO/ppm	Distance (Km)
1	1	9.03	6.2	17
	2	10.3	7.2	18
	3	9.5	6.5	18
	4	10.2	7	18
2	1	7.62	5.6	14
	2	9.4	6.6	16
	3	8.1	6.7	14
	4	8.1	7.2	12
3	1	8.89	6.4	17
	2	9.8	6.9	17
	3	9.4	6.2	18
	4	8.4	7.4	12
4	1	8.3	5.9	16
	2	9.8	7.1	17
	3	8.8	6.3	17
	4	9.1	7.5	15

Table 1: Distance where the low DO concentration was occurring.

Conclusion

Following conclusion and future works can be made as final outcomes based on the results of the current study. Every point has been effect nearby 15km in to the polluted point. Therefore no any kind of effect to the pumping inlet.

In the rainy season high amount of DO concentration is in the water. But in dry season less amount of DO concentration is in the water. Because Oxygen dissolved in water depends on the temperature.

Camper the nitrate and phosphate con centration it shows inverse relationship. It can be change the season wise. In the rainy season there is a high amount of Nitrate concentration in the reservoir. And dry season there is a high amount of phosphate concentration in the water. And also changes in the nitrate and phosphate concentration of the reservoir, change the Algae type in the reservoir.

References

Cox, B.A. (2003). A review of dissolved oxygen modelling techniques for lowland rivers. The Science of the Total Environment 314 –316 (2003) 303–334

Quantum Efficiency (Φ) Enhancement of p-CuI Sensitized LB Films of Methylviolet-C18 by Minimizing Dye Aggregates

P. G. D. C. K. Karunarathna, C. A. N. Fernando

Nano-technology Research Laboratory, Department of Electronics, Faculty of Applied Sciences, Wayamba University of Sri Lanka, Kuliyapitiya, Sri Lanka.

and

S. N. T. De Silva

Department of Biotechnology, Faculty of Agriculture & plantation management, Wayamba University of Sri Lanka, Kuliyapitiya, Sri Lanka.

Introduction

It is well known that the spectral response of wide band gap semiconductor materials can be extended to the visible region by deposition of suitable dyes on the surface (Senadeera et al., 2005; Fernando et al., 2013). In addition to the adustability of the spectral response, dye sensitized solar cells have several advantages (Kubo et al., 2002). The dye sensitized photocurrent is rather insensitive to the impurites and the defects of the semiconductor. When dyes with intense absorption bands are deposited, the light absorption at the sensitized surface becomes much higher than a bare semiconductor surface. Although the absorption properties of the dye increases with the concentration of the absorbed dye on the semiconductor surface, a dye sensitized photocurrent enhacement cannot be observed with the increase of the number of dye molecules on the semicondutor because of the energy dissipative proceses of the excited states of the dye and the recombination of photogenerated charge carriers (Fernando et al., 1994).

Methodology

Commercially available well cleaned copper sheets (1cmx3cm) were used to deposit p-CuI nano thin films from the following method. A solution of CuI was prepared by dissolving 5mg of CuI in 10ml of moisture free acetonitrile. CuI colloidal solution was lightly spread on the well cleaned copper surface until forming a thickness ≈ 5.0 μm to prepare Cu/p-CuI photoelectrodes. Cu/p-CuI photoelectrodes were used to deposit LB films. Experimental set up used for LB deposition is shown in the Fig.1 (Fernando et al., 2013). 2M KI and $1x10^{-2}$M NaH_2PO_4- Na_2HPO_4 pH=6 buffer solution was used as the electrolyte. AFM pictures of the samples were obtained using a Park's AFMXE-70 Instrument. Photocurrent quantum efficiency (Φ%) was calculated using the following equation,

$$\Phi\% = [\text{number of electrons created} / \text{number of photons incident}] \times 100\% \qquad (1)$$
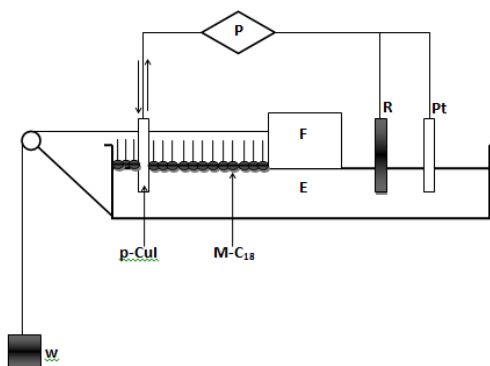
Fig.1 P- Potentiostat   R- Reference Electrode Pt- Platinum counter electrode E- Electrolyte F-Floater W- Weight

Results and Discussion

Fig.2 shows the AFM micrographs of M-C18 LB films deposited on conductive glass plates at +0.3V vs AgCl/Ag. In case of the films deposited on glass plates at +0.3V show a homogeneous surface morphology as shown in the figure. Formation of the homogeneous surface morphology may be due to the formation of ordered monomer molecular arrangement.

Fig.3 and Fig.4 show the variation of the photocurrent quantum efficiency with number of M-C_{18} LB monolayers deposited on p-CuI at different applied potentials. It is clearly seen an enhancement of the photocurrent occurs with the LB films deposited potentials are more possitive. Further an optimum surface concentration can be observed in each case. It is interesting to mention that the optimum surface concentration of M-C_{18} LB films increases when the deposition applied potential increases towards possitive side enhancing the maximum photocurrent quantum efficiencies. Table-1 shows the variation of maximum photocurrent quantum efficiency ($\Phi_{max}\%$) with LB deposition applied potential. Maximum photocurrent quantum efficiency reached was $\approx$ 22% at +0.3V vs AgCl/Ag .
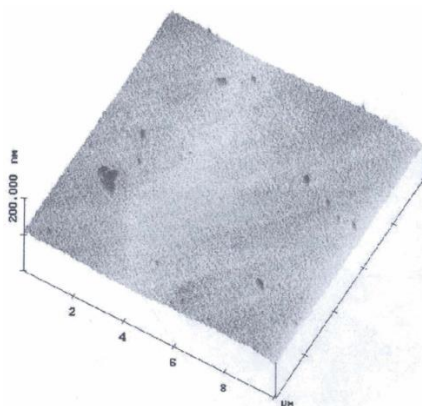
Fig.2 AFM image for the 18 monolayers of C_{18}-MERO-C_{18} LB films prepared at +0.3V vs Ag/AgCl applied potential

25
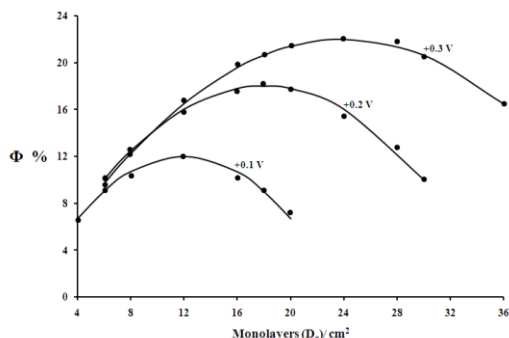
Fig.3 The varition of photocurrent quantum efficiency ($\Phi\%$) with number of M-C_{18} Monolayers deposited at different possitive applied potentials in the presence of (10^{-3}M) Fe^{2+} /Fe^{3+} (10^{-3}M) at $\lambda = 560$nm

Table 1: Optimum number of monolayer / optimum photocurrent quantum efficiency at different applied potential.

Applied Voltage (V)	D_{op} (cm^2)	$\Phi_{Max}\%$
+0.1	12	12
+0.2	18	18
+0.3	24	22

Conclusions

Photocurrent quantum efficiencies for both PECs and DSSCs are increased for the LB films of M-C_{18} prepared at positive biased potentials minimizing the formation of M-C_{18} dye aggregates. The power conversion efficiency reached for DSSC is 2% for the films deposited at +0.3V vs Ag/AgCl. Photocurrent quantum efficiencies for the p-CuI/M-C_{18} photoelectrode are increased for the LB films of M-C_{18} prepared at positive biased potentials minimizing the formation of M-C_{18} dye aggregates.

Acknowledgement

References

Fernando, C.A.N., Kitagawa, A., Suzuki, M. & Takahashi, K.a.K.T., 1994. *Sol. Energy Mater and Sol. Cells*, 33, p.301.

Fernando, C.A.N., Liyanaarachchi , U.S. & Rajapaksha, R.D.A.A., 2013. *Semicond. Sci. Technol*, 28.

Kubo, W. et al., 2002. *Chem. Commun.*, p.374.

Senadeera, G.K.R. et al., 2005. *Bull. Mater. Sci.*, 28, p.635.

Relating climatic parameters with leachate chemistry and its association with river water quality

W.M.D.S.K. Weerakoon
Faculty of Science and Technology, Uva Wellassa University of Sri Lanka

Dr.S.K.Weragoda
National Water Supply and Drainage Board

and

Dr.C.S.K.Kalpage, Dr A.M.Ziyath and Dr A.Manipura
Faculty of Engineering, University of Peradeniya, Sri Lanka
.

Introduction

Increased solid waste generation due to rapid urbanization and industrialization is a major problem in the world (Golomeova et al. 2013). .Landfilling is the most common disposal method of municipal solid waste (MSW) in developing countries, even though majority of these landfills are not properly managed, and pose a serious threat to the environment due to leachate run-off which contaminates the nearby ground water and surface water bodies (Kjeldsen 1993).

The quantity and quality of leachate is influenced by various factors and climatic conditions are one of these governing factors (Chu et al. 1994; Johansen & Carlson 1976). Hence this study was carried out focusing on the impact of climatic parameters on leachate quality and its association with the Mahaweli river water quality which has not yet been further studied. Meantime two main objectives were fulfilled during the process of reaching the main target. They were, investigating seasonal variation of leachate chemistry and Mahaweli river water quality and developing correlation between climatic parameters, leachate chemistry and Mahaweli river water quality.

Materials and methods

Landfill leachate ,river water samples and ground water samples were collected from the leachate drain of the Gohagoda landfill, four locations along the Mahaweli river- two upstream and two downstream points from where leachate drain to the river and from two wells within the landfill. Weekly sampling was carried out for a period of two months and sample preservation, storage and analysis were performed according to Standard Methods (APHA, 1999). Daily temperature and rainfall data were collected from Horticultural Crop Research and Development Institute (HORDI) Gannoruwa and the statistical computations were performed with MINITAB version 17.0.

Results and Discussion

All the measured leachate and water quality data are summarized in Table 1.As the first step, primary leachate characteristic values were being compared with the past studies (Wijesekara et al.) and with the recommended standards of tolerance limits for discharge of effluent for inland surface waters by the Central Environmental Authority (CEA). Alkaline pH value represented the methanogenic stage of the landfill(More than 10y of operation) and exceed the CEA value. TDS and EC values of the leachate were very high (1.33×10^4 mg/L & 2.05×10^4 μs/cm) compared to other sites. Dissolved Oxygen showed a very low value (0.09 mg/L) at the leachate drain owing to the anaerobic conditions and oxidisable organic matter related components are measured as BOD and COD. Both of these components were exceeding the CEA values. BOD:COD ratio was stated as 0.911 representing acidogenic condition which contrast with the above results. It is obvious that the uncontrolled dumping of the waste can produce leachate with various ages due to the irregular degradation pattern of the refuse material.(Wijesekara et al).

According to the study, 5.24×10^2 mg/L of TOC is present in the Gohagoda leachate once more endorse the high organic concentration of the leachate. Nitrate-nitrogen (63.33mg/L) and Phosphate (23.67mg/L) concentrations have exceeded the CEA limits. The nitrate of the leachate is mainly from biological sources, human and animal excreta accounting for a large percentage of the total nitrogen load. Furthermore, Cadmium concentration was below the SLS standards

First step of assessing the impact of leachate on river water quality was based on ANOVA tests. Significant difference in any of the parameters between river water upstream (U1 & U2) and downstream (D1 & D2) of the point where leachate entered the river were checked. According to the results TOC showed significant differences among all locations at 5 % probability level ($P< 0.05$)

Furthermore, correlation analysis was performed in order to study the impact of leachate (L) on river and ground water quality (D1,D2,W1,W2 & M).High positive correlation ($0.5 < r < +1$) was obtained between Inorganic Carbon (L-M), Phosphate (L-W1),Ammonia(LD2 & LW2),Cd(LD2-LM).This can further confirm the observation obtained from the ANOVA table which pointed out that there was an impact of leachate on downstream water quality. Dissolve Oxygen concentration of leachate had an weak positive correlation ($0 < r < 0.5$) with all the interested points.(L,M,D1,D2,W1,W2). Similar relationship was obtained for Nitrate, Ammonia, IC,TOC and Cadmium between leachate and Well 1.Well 2 showed the same pattern of relationship for IC,TOC and Phosphate.D1 and leachate showed weak positive relationship of IC and D2 showed for Phosphate. All other relationships were highly or weakly correlated.

Correlation between climatic parameters and leachate chemistry was studied using Pearson Correlation. According to the Pearson correlation, pH has a high positive correlation with the temperature and a weak positive correlation with the rain fall. . Dilution occur at the rainy days may cause the weak positive correlation with the rain fall. At the same Electrical conductivity and the total dissolved solids show a strong positive relationship with the temperature and these two parameters show weak negative relationship with the rainfall. According to the literature,

(Maqbool et al.2011) low DO values were reported at high temperature which contrasts with correlation results obtained from the present study.

 Rest of the parameters (COD,BOD,TC,TN,IC,TOC Phosphate,Nitrate,Ammoia and Cadmium) shows a negative correlation with the temperature. TC,TN,IC,TOC,Phosphate,and Ammonia shows a negative relationship with the rainfall most probably due to dilution.

Conclusions.

The concentrations of Gohagoda landfill leachate components in the primary leachate were higher than CEA standard values and most of these parameters were similar to the past studies. According to the results obtained from the Pearson correlation Analysis and the ANOVA table, no significant impact on Mahaweli river water was caused by the Gohagoda leachate and this is most probably based on the dilution Few of the leachate parameters were effected from the temperature and rainfall, yet a comprehensive study should be carried out encountering all other climatic parameters(wind pattern, solar radiation) in order to develop a broad view.

References
Chu, L. M., Cheung, K. C. and Wong, M. H.: 1994, 'Variations in the chemical properties of landfill leachate', *Environ. Manage.* 18, 105–117.

Golomeova, Saska, et al. "Solid waste treatment technologies." Machines, Technologies, Materials 9 (2013): 59-61.

Kjeldsen, P., Barlaz, M. A., Rooker, A. P., Baun, A., Ledin, A., & Christensen, T. H. (2002). Present and long-term composition of MSW landfill leachate: a review. *Critical reviews in environmental science and technology*, *32*(4), 297-336.

Wijesekara, S. S. R. M. D. H. R., Mayakaduwa, S. S., Siriwardana, A. R., de Silva, N., Basnayake, B. F. A., Kawamoto, K., & Vithanage, M. Fate and transport of pollutants through a municipal solid waste landfill leachate in Sri Lanka. *Environmental Earth Sciences*, 1-13.

Table 01.Summery of the leachate river water and ground water quality data

Parameter	Unit	(L)	(M)	(U1)	(U2)	(D1)	(D2)	(W1)	(W2)
pH		8.57 ± 0.3	7.99 ± 0.3	7.66 ± 0.6	7.78 ± 0.5	7.76 ± 0.4	7.77 ± 0.6	6.81 ± 0.4	7.57 ± 0.7
		$8.36 - 8.96$	$7.6 - 8.4$	$6.97 - 8.48$	$7.33 - 8.68$	$7.06 - 8.53$	$7.37 - 8.62$	$6.31 - 7.66$	$6.96 - 8.62$
Electriacal Conducti	$\mu s/cr$	$2.05^*10^4 \pm 3.24^*10^3$	$1.62^*10^2 \pm 1.7^*10^3$	64.2 ± 26.7	73.24 ± 29.3	67.33 ± 12.04	88 ± 18.19	$3.88^*10^2 \pm 3.5^*10^1$	$5.36^*10^2 \pm 1.3^*10^2$
		$1.53^*10^4 \pm 2.42^*10^4$	$52 - 5110$	$11.2 - 96.0$	$46.7 - 135$	$53 - 83.3$	$61.8 - 114.6$	$3.27^*10^2 - 4.48^*10^2$	$2.94^*10^2 \pm 6.18^*10^2$
Dissolved Oxygen	mg/L	0.09 ± 0.4	3.61 ± 3.3	7.66 ± 0.3	7.61 ± 0.2	7.61 ± 0.2	7.5 ± 0.4	5.26 ± 1.9	6.24 ± 1.1
		$0.06 - 0.16$	$0.55 - 4.66$	$7.28 - 8.43$	$7.31 - 7.96$	$7.31 - 7.96$	$7.11 - 8.23$	$7 - 18$	$4.2 - 7.44$
Total Dissolved Soli	mg/L	$1.33^*10^4 \pm 2.2^*10^3$	$7.5^*10^2 \pm 1.1^*10^3$	48.5 ± 13.4	53.59 ± 19.0	53.59 ± 19.0	54.83 ± 15.28	$2.56^*10^2 \pm 2.^*10^1$	$4.18^*10^2 \pm 6.6^*10^1$
		$9.9^*10^3 - 1.6^*10^4$	$1.33^*10^2 - 3.37^*10^3$	$31.4 - 74.0$	$31.7 - 89.1$	$31.7 - 89.1$	$35.8 - 76.1$	$2.15^*10^2 - 2.96^*10^2$	$3.78^*10^2 - 5.79^*10^2$
Sulphate	mg/L		11 ± 16.4	1 ± 0.76	0.88 ± 0.8	1 ± 0.6	2 ± 1	9.5 ± 2	37.75 ± 1.75
			$0 - 40$	$0 - 2$	$0 - 2$	$0 - 2$	$1 - 3$	$04-Jul$	$35 - 40$
Posphate	mg/L	23.67 ± 6.4	14.49 ± 9.8	0.23 ± 0.1	0.24 ± 0.1	0.51 ± 0.7	0.25 ± 0.01	0.44 ± 1.4	3.43 ± 8.31
		$15 - 32$	$0.66 - 25$	$0.07 - 0.37$	$0.1 - 0.53$	$0.19 - 2$	$0.23 - 0.27$	$0.17 - 0.61$	$0.14 - 24$
Nitrate-Nitrogen	mg/L	63.33 ± 17.5	55.38 ± 24.72	1.13 ± 0.4	0.98 ± 0.2	6.94 ± 0.5	1.22 ± 0.3	1.47 ± 0.87	6.84 ± 1.27
		$40 - 90$	$Mar-90$	$0.4 - 1.7$	$0.5 - 1.2$	$0.3 - 1.6$	$0.8 - 1.5$	$1 - 3.6$	$4.3 - 7.9$
Ammonia-Nitrogen	mg/L	$1.35^*10^3 \pm 8.6^*10^2$	$3.99^*10^2 \pm 5.5^*10^2$	0.65 ± 0.6	3.08 ± 6.9	0.42 ± 0.4	1.01 ± 1.6	1.89 ± 4.5	0.63 ± 0.16
		$1.1^*10^2 - 2.8^*10^3$	$1.86 - 1370$	$0.4 - 1.7$	$0.13 - 20$	$0 - 1$	$0.17 - 3$	$0.08 - 13$	$0.43 - 0.9$
Total Nitrogen		$1.4^*10^3 \pm 8.6^*10^2$	$3.41^*10^2 \pm 3.6^*10^2$	2.1 ± 1.4	6.20 ± 11.7	19.16 ± 32.9	4.15 ± 6.9	1.85 ± 4.9	6.86 ± 3.04
		$3.37^*10^2 - 2.35^*10^3$	$44.19 - 460.5$	$0.96 - 4.93$	$1.19 - 30.17$	$2.28 - 85.91$	$9.66^*10^{-2} - 1.8^*10^1$	$0.45 - 3.34$	$1.69 - 9.76$
Cadmium		$4.1^*10^{-3} \pm 2.4^*10^{-3}$	$3.4^*10^{-2} \pm 7.6^*10^{-2}$	$8.4^*10^{-3} \pm 1.3^*10^{-2}$	$2.3^*10^{-3} \pm 1.4^*10^{-2}$	$1.64^*10^{-4} \pm 6^*10^{-3}$	$3^*10^{-3} \pm 1^*10^{-3}$	$1.42^*10^{-3} \pm 9.5^*10^{-4}$	$3.6^*10^{-3} \pm 3.2^*10^{-3}$
		$1.8^*10^{-3} - 8.2^*10^{-3}$	$1.3^*10^{-3} - 1.9^*10^{-1}$	$3^*10^{-4} - 2.86^*10^{-2}$	$6^*10^{-4} - 4.5^*10^{-3}$	$1^*10^{-3} - 2.4^*10^{-3}$	$0 - 8.1^*10^{-3}$	$0 - 2.4^*10^{-4}$	$7^*10^{-4} - 9^*10^{-3}$
BOD	mg/L	$1.57^*10^2 \pm 1.8^*10^2$		7.25 ± 4.98	6.62 ± 1.2		31.12 ± 39.1	11.63 ± 8.86	
		$266 - 573$	$13 - 465$		43525	$4 - 8$		$8.59 - 119.3$	$5 - 33$
COD	mg/L	$474.83 \pm 2.2^*10^3$							
		$931.1 - 5840$							
Total Organic Carbo	mg/L	523.9 ± 47.73	$4.98^*10^2 \pm 3.7^*10^2$	3.82 ± 1.1	12.72 ± 11.61	1.88 ± 1.7	7.34 ± 7.01	19.34 ± 39	9.94 ± 11.54
		$18.5 - 952.1$	$1.39^*10^2 - 1.14^*10^3$	$2.57 - 5.87$	$3.33 - 31.25$	$4.4^*10^2 - 4.75$	$2.56 - 21.42$	$2.37 - 16.32$	$2.21 - 33.14$
Total Carbon	mg/L	$3.16^*10^3 \pm 2.2^*10^3$	$1.36^*10^3 \pm 1.5^*10^3$	8.02 ± 1.9	23.09 ± 24.88	10.06 ± 3.69	13.63 ± 10.8	10.35 ± 4.9	40.66 ± 15.3
		$9.31^*10^2 - 5.84^*10^3$	$167.2 - 402.1$		319	$6.62 - 16.13$	$5.4 - 35.3$	$2.37 - 16.32$	$7.74 - 63.24$
Inorganic carbon	mg/L	$1.73^*10^3 \pm 1.2^*10^3$	$2.29^*10^2 \pm 4.2^*10^2$	4.11 ± 1.2	10.36 ± 16.13	4.07 ± 1.15	6.28 ± 4.08	10.35 ± 4.93	33.2 ± 12.2
		$5.37^*10^2 - 3.3^*10^3$	$28.1 - 1076$	$2.84 - 6.63$	$3.39 - 46.91$	$1.88 - 5.32$	$2.84 - 13.86$	$2.37 - 16.32$	$5.52 - 44.55$

Determination of potential use of chitosan for the removal of Pb, Fe and Mn in the water samples collected from different areas of Sri Lanka

S. Farhan

Department of Science and Technology, Uva Wellassa University, Sri Lanka.

and

S.M. De Silva, C.S.K. Rajapakse
Department of Chemistry, University of Kelaniya, Sri Lanka.

Introduction

Water contamination is one of the major concerns in the world. From the beginning of the 21st century, the drinking water sources in the main agricultural regions under reservoir based irrigation of Sri Lanka have been polluted from heavy metals in considerable amounts and exposure to heavy metals can cause a number of health problems, ranging from nausea and stomach discomfort to development of cancers and kidney diseases (Bandara *et al.,*2008). Although a wide range of physical and chemical processes are available for the removal of heavy metals from natural water bodies, most of these methods are not practicable to developing country like Sri Lanka as they are extremely expensive. In recent years, biosorption has been recognized as an effective method of removal of heavy metal contaminants in surface water as low cost bio-adsorbents are readily available, environmentally friendly, and biodegradable. The bioadsorbent chitosan; deacetylated product of chitin (Gamage *et al.,*2007) has been used as a bioadsorbent for the removal of toxic/heavy metals from waste water. Depending on the pH of the medium the interaction of metals with chitosan are possibly dominated by adsorption, ion-exchange and chelation. Chitosan has been used to remove heavy metals mainly from industrial wastewater and as a non-toxic flocculent in the treatment of organic polluted wastewater (Shanmugapriya *et al.,* 2011); but little attempt has been made to understand the ability of chitosan to uptake heavy metals in polluted drinking water containing trace amounts (ppb levels) of heavy metals (De Silva *et al.,*2014).

The current study focuses on potential of using chitosan as a low cost, environmentally friendly biosorbent for purification of drinking water contaminated by the low levels of heavy metal pollutants; Pb, Fe and Mn.

Methodology

Drinking water samples were collected from different areas of the country including Anuradhapura, Nikkawewa, Vavuniya, Trincomalee, Badulla and Kantale. First the basic parameters such as colour, pH and total hardness of the collected water samples were measured and recorded. Then the initial metal ion concentration of Pb, Fe and Mn of acid digested water samples were measured using AAS.

Next, all the water samples with initial metal ion concentrations above the permissible limits for drinking water defined by the World Health Organization (WHO) were treated with chitosan as follows. A finely crushed chitosan (0.0250 g) was taken separately into clean dry polypropylene containers. A volume (50.00 mL) of digested water sample was introduced into polypropylene container having chitosan sample. pH of the sample was adjusted to pH 7 using NaOH (0.1 M) and the sample container was stirred at room temperature (29.0 ± 0.5 ºC) for 2 hours. Control sample was prepared simultaneously with chitosan (0.0250 g) and deionized water (50.00 mL) and pH was adjusted to pH 7. Control sample was also stirred at room temperature (29.0 ± 0.5 ºC) for 2 hours. After 2 hours stirring period, both sample and control were filtered using filter papers. Filtrates of sample and control were analyzed by AAS to determine the amount of Pb, Fe, and Mn remaining in the solutions after treatment with chitosan. The procedure was carried out in duplicate for each digested drinking water sample.

Result and Discussion

The pH values of the collected water samples range from 6.53 – 7.31 which were in the range of accepted pH value range (6.5 – 8.5) for drinking water defined by WHO. But hardness in some of the collected water samples had exceeded 250 ppm, the maximum permissible level defined by the Sri Lanka Standards Institution (SLSI) for the drinking water.

The Initial metal concentrations in collected water samples, metal concentrations after treatment with chitosan, and percentage metal removal (%) of Pb Fe and Mn are shown in table 1, table 2 and table 3 respectively. The maximum permissible levels for drinking water given by WHO for corresponding metals are shown in table 4.

Table 1: Concentration of Pb in water samples - before and after treatment with chitosan.

Sample No	Water Sample	Concentration of Pb (µg/L)		% removal
		Before treatment	After treatment with chitosan	
01	Vavuniya Tank 01	19.50 (±0.13)	6.26 (±0.12)	67.89
02	Vavuniya Tank 02	22.12 (±0.06)	7.61 (±0.04)	65.59
03	Vavuniya Tank 03	14.62 (±0.24)	5.70 (±0.08)	61.01
04	Vavuniya Tank 04	17.15 (±0.11)	6.92 (±0.22)	59.65
05	Vavuniya Well	20.62 (±0.04)	8.34 (±0.14)	59.55
06	Paththawewa Tank	15.72 (±0.07)	8.76 (±0.03)	44.27
07	Wepannkulam Tank	12.14 (±0.03)	7.72 (±0.31)	36.41
08	Anuradhapura Well 1	18.72 (±0.16)	9.76 (±0.14)	47.86
09	Nikkawewa Well	16.41 (±0.02)	7.36 (±0.20)	55.15
10	Kantala Tank	13.25 (±0.12)	5.27 (±0.03)	60.23

Table 2: Concentration of Fe in water samples - before and after treatment with chitosan.

Sample No	Water Sample	Concentration of Fe (μg/L)		% removal
		Before treatment	After treatment with chitosan	
01	Paththawewa Tank	385.00 (±0.05)	115.30 (±0.03)	70.05
02	Nikawewa Tank	879.00 (±0.04)	270.50 (±0.12)	69.23

Table 3: Concentration of Mn in water samples - before and after treatment with chitosan.

Sample No	Water Sample	Concentration of Mn (μg/L)		% removal
		Before treatment	After treatment with chitosan	
01	Paththawewa Tank	1003.00 (±0.13)	270.00 (±0.08)	73.08
02	Wepannkulam Tank	827.00 (±0.04)	255.50 (±0.23)	69.11

Table 4: Maximum permissible levels given by WHO for Pb, Fe and Mn.

Metal	Maximum permissible level/ μg/L
Lead (Pb)	10
Iron (Fe)	300
Manganese (Mn)	400

According to the results, all the water samples with higher levels of Pb, Fe and Mn concentrations were successfully reduced into the permissible range defined by WHO by treating with biopolymer chitosan.

Conclusion

Interestingly, all the water samples with initial metal ion concentrations above the permissible limits were successfully reduced into the permissible range defined by WHO by treating with chitosan, further proved that chitosan might be a good candidate which can be used to remove heavy metals from polluted drinking water. The average percentage removal of lead, iron and manganese by chitosan is 55.77% 69.65% .and 69.60% respectively.

References

Bandara, J.M.R.S., Senevirathna, D.M.A.N., Dasanayake, D.M.R.S.B., Herath, V., Bandara, J. M.R.P., Abeysekara, T.K., Rajapaksha, H. (2008). Chronic renal failure among farm families in cascade irrigation systems in Sri Lanka associated with elevated dietary cadmium levels in rice and freshwater fish (*Tilapia*). Environmental Geochemistry and Health, 30(5), 465-478.

De Silva, S.M., Fernando, W.T.I., Kannangara, A.T., Ubesena, J.G.P.S., Rajapakse, C.S.K. (2014). Determination of heavy metal adsorption capacity of chitosan and removal of heavy metals from drinking water using chitosan. Proceedings of Third International Symposium on Water Quality and Human Health: Challenges Ahead, Postgraduate Institute of Science (PGIS), University of Peradeniya, Sri Lanka. pp. 37.

Gamage, A., Shahidi, F. (2007). Use of chitosan for the removal of metal ion contaminants and proteins from water. Food Chemistry, 104, 989–996.

Shanmugapriya, A., Ramya, R., Ramasubramaniam, S., Sudha, P. N. (2011). Studies on removal of Cr(VI) and Cu(II) ions using chitosan grafted-polyacrylonitrile. Archives of Applied Science Research, 3(3), 424-435.

Heavy metals and trace element distribution in Eppawala Apatite deposit

P.C.B.Wickramsinghe and D.T. Udagedra

Uva Wellassa University, Badulla, Sri Lanka

D.T. Jayawardana

Faculty of Applied Sciences, University of Sri Jayewardenepura, Nugegoda, Sri Lanka

Introduction

In Sri Lanka, the dominant source of drinking water used to supply major urban and rural communities is from wells, tanks, rivers, springs. Although there are no systematic and comprehensive water quality assessment programs in the country, there are increasing indications of water contamination problems in some parts of the country. Causes for water contamination are natural or anthropogenic. Among natural contamination, water-rock interaction is critical but remains hidden for most eyes. No sufficient study has been conducted on heavy metal contamination of drinking water of the Eppawala apatite area in Sri Lanka. The main objective of this paper is to determine the influence of some of the physicochemical parameters and heavy metals and trace elements in drinking water and its distribution of different parts of the Eppawala.

Methodology

The groundwater was studied around the Eppawala Apatite Deposit (EPD) using tube well and dug wells as the access. Sample size (60) was determined by distribution of the population around the EPD. Samples were collected in wet season and dry season. The electrical conductivity was measured in situ with Orion 3 Star EC meter. The collected water samples were analyzed for seventeen (17) parameters including major cations, anions, heavy metals and trace elements. Cations, heavy metals and trace elements concentration with the Varian SpectrAA AAS facility available at the Uva Wellassa University. Anions including SO_4^{2-}, Cl^- and HCO_3^- were measured using standard methods. The major cations such as Ca, Cu, Fe, K, Mg, Mn, Na, Zn, Cs, Sr, Li, Rb, and major anions such as SO_4^{2-}, Cl^- , F^- and HCO_3^- were analyzed using the ORIGIN 8 and Surfer software.

Results and discussion

In terms of electrical conductivity, it ranged from 19.2ms/cm-1.02ms/cm in wet season and 1.75ms/cm-0.32ms/cm in dry season. Normally Na^+, Mg^{+2}, F^- and Cl^- are the highly abounded elements in the selected area well water in wet season. That's value are above the Sri Lankan drinking water stranded.

Table 01: Highly effected elements in the wet season collected samples

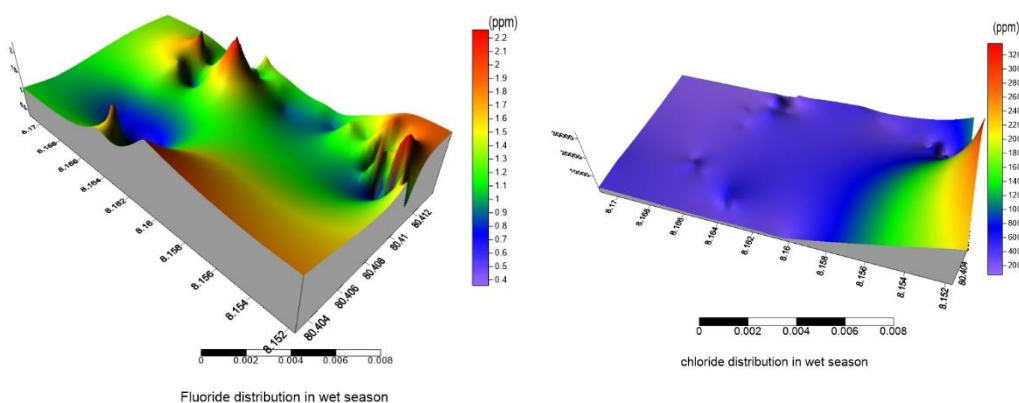| Parameter	Mean value (ppm)	Drinking water standard level (ppm)
Chloride (Cl-)	3270	1200
Fluoride (F-)	1.31	1
MagnesiumMg^{2+}	158	150

Figure: 1 Fluoride and Chloride distribution in wet season

Furthermore, there is a highly vary Mn^{+2} in both wet and dry season(mean value 0.007ppm and 0.1ppm) As well as Li (mean value 0.003ppm and 0.015ppm). In table 02 and 03 are summarized the all parameters in wet and dry season.

Table 02: Elements analyzed results of wet season

Parameter	Mean value	Standard deviation	Range
pH	7.9	7.5	6.1 – 8.2
Conductivity(mc/cm)	2.87	2.57	19.2 - 1.02
Chloride (Cl$^-$)	3270.17 ppm	1969.4	9633.8 – 772.4
Fluoride (F$^-$)	1.31 ppm	0.56	2.2 – 0.16
Bicarbonate (HCO^{-3})	205.7 ppm	81.77	439.2 – 48.8
Phosphate (PO$_4$-^{3})	0.42 ppm	0.129	1.10 – 0.211
Sulphate (SO$_4$$^{-2}$)	1.11 ppm	0.51	3.14 – 0.42
Calcium (Ca^{+2})	145.57 ppm	154.69	1100 – 31.9
Cesium (CS^{+1})	0.68 ppm	0.56	1.74 – -0.37
Cupper (Cu^{+2})	0.037 ppm	0.016	0.013
Ferrous (Fe^{+2})	-0.009 ppm	0.018	0.065 - -0.024
Potassium (K^{+1})	2.17 ppm	1.38	8.85 – 0.65
Lithium (Li^{+1})	0.003 ppm	0.004	0.003 - 0
Magnesium (Mg^{+2})	158.58 ppm	89.19	608.79 – 52.75
Sodium (Na^{+1})	383.56 ppm	238.24	1000 – 64.64
Manganous (Mn^{+2})	0.007 ppm	0.019	0.15 - -0.003
Rubidium (Rb^{+1})	0.397 ppm	0.113	0.689 – 0.044
Strontium (Sr^{+2})	1.90 ppm	0.99	5.12 – 0.037
Zinc (Zn^{+2})	0.013 ppm	0.022	0.132 – 0.003

Table 03: Element analyzed results of dry season

Parameter	Mean value	Standard deviation	Range
pH	7.28	0.245	7.85 – 6.85
Conductivity	0.87 ms/cm	0.394	1.75 – 0.32
Lithium (Li^{+1})	0.015 ppm	0.006	0.026 – 0.005
Manganous (Mn^{+2})	0.1 ppm	0.196	0.621 – 0.051
Rubidium (Rb^{+1})	0.232 ppm	0.033	0.271 – 0.168
Strontium (Sr^{+2})	2.831 ppm	1.098	5.298 – 1.002

Conclusion

According to the results, heavy metals and trace elements concentration are changing seasonally. Most of the heavy metal and trace element in groundwater around EPD are not exceed Sri Lanka drinking water standard level. Chloride (Cl^-) is the highly abundant elements in the groundwater in the selected area (mean Cl^- concentration is 3270.17 ppm). According to the Sri Lankan drinking water standard Cl^- should be below the 1200 ppm. Fluoride (F^-) is highly present in the water sample (1.31 ppm). According to the Sri Lankan drinking water standard F^- level should less than 1 ppm. It is the big problem in this sample collected area.

References

Anderson, S.P., Dietrich, W.E. and Brimhall, G.H., (2002). Weathering profiles, mass-balance analysis, and rates of solute loss: Linkages between weathering and erosion in a small, steep catchment. Geol. Soc. America Bulletin Vol. 114, p. 1143-1158.

Environment Management, Director, 2011. Sri Lanka Standards for potable water – SLS 614, 1983. 1st ed. Sri Lanka: Board of Investment.

Determine the Presence of Gold and its Distribution in Upper Nilwala River Basin, Southern Part of Sri Lanka

B.G.P.T.Saranga, J. T. Cooray,
Faculty of Science and Technology, Uva Wellassa University of Sri Lanka

S. Siriwardhane and W.K.B.N.Prame
Geolological Survey and Mines Bureau, Pitakotte, Sri Lanka

Introduction

Gold (Au) is a chemical element, bright yellow dense, soft, malleable and ductile metal. The properties remain when exposed to air or water. It occurs often in free elemental (native) form, as nuggets or grains, in rocks, in veins and in alluvial deposits.

Investments made on gold prospecting are only second to oil exploration. This research was carried out to find gold in upper Nilwala River and possible areas that gold can be found. In this study, distributions of indicator elements of gold were studied to identify potential gold enrichments in the upper Nilwala River Basin.
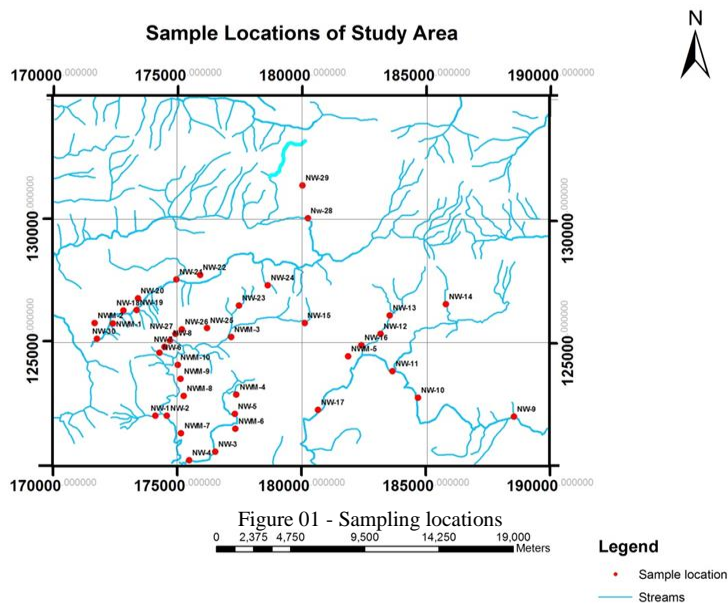
Materials and methods

Figure 01 - Sampling locations

Stream sediment samples were collected mainly from the placer deposits see figure 1. Samples were taken at about 1 –2 feet depth on placer deposit or river bed by using a shovel. Also gem pit sediment samples were collected near to the gem bearing layer. Samples were collected using the hand pit method (Fletcher *et al.*, 1997). A total of 1–2 kg of raw samples was taken from each location. Then all samples were transferred to neatly labeled polyethylene bags. About 1 kg of sediment samples were separated by using cone and quarter method. Then heavy sediments of it were separated by panning method . Then it was dried in a hot air oven. Each sample was stored in a labeled sample bags to use for mineralogical analysis carried out using an optical microscope. From remaining dried 1 kg samples were homogenized and near 100 g of samples were again separated using cone and quarter method. Then separated sample fractions were crushed by using vibrating cup mill to less than 63 µm.

Optical microscope was used to identify the minerals occur in the heavy sediment sample. Using corn and quarter method substantial amount of heavy sediments were separated for the testing. Using a magnet all the magnetic minerals of the sample was separated. 5X5 equal squares were marked on the glass slid. Then glycerol liquid was applied on the top of that slid. After that heavy sediments were put on to the slid creating a fine layer. Finally both magnetic and nonmagnetic minerals were analyzed. Couples of samples were selected. Magnetic separation was done for those samples. Then for the nonmagnetic section Bromoform test was done. Then the heavy particles were separated. After that the samples were analyzed using an optical microscope.

The grinded sediments (<63 µm) were tested using X-ray florescence spectroscopy (XRF) to identify chemical composition and major elements for each sample.

Results and Discussion

XRF results of the samples show the gold occurrence at five locations. Gold concentration is shown in bellow table 1.

Table 01: The gold concentration in gold found areas.

Sample No	Gold Amount/ppm
NW-2	75
NW-8	15
NWM-4	45
NWM-8	1375
NWM-10	5145

Gold nuggets were observed under the microscopic survey where the highest gold concentration observed for XRF see figure 2.
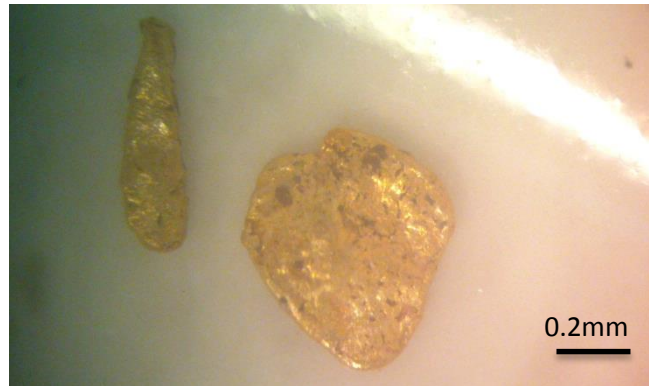
Figure 2 - Gold Nuggets observed at NWM-10.

Six major indicator minerals of gold were selected. Those are As, Pb, Se, Co, Ni and Cu. Bellow table shows sample locations which have highest indicator minerals,

Table 02: Highest amount of indicator element found areas with their indicator minerals.

Sample No	Indicator Elements
NWM-5	As, Se, Ni, Cu
NWM-6	As, Se, Ni, Cu
NW-23	As, Ni, Cu
NW-28	Se, Co, Cu
NWM-1	Pb, Ni, Cu
NWM-9	As, Ni, Co

Therefore it can be inferred that gold can be found at these sample locations as well.

Conclusions

This study reveals the enrichment of gold at several locations in the upper Nilwala River basin. Gold present in these areas mainly in the form of dust and small nuggets. There is a high possibility to find gold in sample location NWM-5, NWM-6 and in sample NW-23, NW-28, NWM-1 and NWM-9.

Acknowledgement

References

Fletcher, W.K. (1997). Stream sediment geochemistry in today's exploration world. Exploration Geochemistry, 32, 1-3. Retrieved may 22, 2014, from the World Wide Web: http://www.dmec.ca/ex07dvd/Decennial%20Proceedings/Expl97/03_05___.pdf

Geochemistry and Mineralogy of Chaliyar river sediments with special reference to the occurrence of placer gold. Retrieved from the World Wide Web: http://dyuthi.cusat.ac.in/purl/34

Magnesium rechargeable cells based on PVdF gel polymer electrolyte

Y.M.C.D. Jayathilake, K.S. Perera and K.P. Vidanapathirana

Department of Electronics, Wayamba University of Sri Lanka, Kuliyapitiya Sri Lanka

Introduction

Gel polymer electrolytes (GPEs) have received a keen interest as an excellent substitute for liquid electrolytes due to anticipation of several advantages such as no leakage, no corrosion and easy preparation. They are basically consisting of a salt solvent mixture encapsulated in a suitable polymer matrix (Osman, *et al.* 2012). Due to the satisfactory conducting and mechanical properties, they have been extensively considered as suitable electrolytes for various applications such as rechargeable cells (Kumar *et al*, 2003) super capacitors (Tripathi *et al*, 2013) and electrochromic devices (Wu *et al*, 2012). Plentiful of investigations have been carried out on applications with Li based GPEs but now attention has been focused towards other cation based GPE mainly due to some problems associating with lithium. As such non lithium based devices have come forward getting more interest. Use of magnesium in place of lithium would be very convenient as it possesses various important characteristics such as low cost, substantial abundance, more stability than lithium and low toxicity (Pandey *et al*, 2011). This paper reports about employing a magnesium based GPE in a magnesium rechargeable cell.

Methodology

Polyvinylidenefluoride (PVdF), Ethylene carbonate (EC), Propylene carbonate (PC) and Magnesium trifluromethane sulfonate (MgTf) purchased from Aldrich were used as received. Appropriate amounts of EC, PC and MgTf were mixed by magnetically stirring for about 2 hours. Required amount of PVdF was added and stirring was continued for another 10 minutes. Then, the mixture was heated at 120 ^{0}C for 30 minutes. The resultant homogenous hot mixture was pressed in between two well cleaned glass plates to obtain a thin GPE film. A circular pellet of GPE was sandwiched in between two stainless steel (SS) electrodes and it was loaded inside a brass sample holder which is sealed by means of an O ring. Diameter and thickness of the sample were measured using a micrometer screw gauge. AC Impedance data were gathered by using Metrohm Autolab M101 impedance analyzer in the frequency range 0.01 Hz - 0.1 MHz. Temperature was varied from room temperature to 60 ^{0}C by placing the sample holder inside a Sibata glass tube furnace. Cyclic Voltammetry studies were performed by placing an electrolyte sample in between two Mg electrodes. Three electrode electrochemical setup with a working electrode, a counter electrode and a reference electrode was employed for the study. Scan rate

used was 5 mV/s. A cathode having Polypyrrole (PPy) polymerized in the presence of Dodecylbenzenesulfonate (DBS) was prepared as reported before (Perera *et al,* 2008). The cells in the configuration, Mg / GPE / PPy : DBS were assembled and their charge discharge behavior was monitored. Cells were subjected to charge and discharge between the potential values 0.5 V and 2.0 V. They were first discharged galvanostatically and then charged galvanostatically. When the required potential has reached, further potentiostatic charge was done till the current drops to 10%.

Results and Discussion

 The selected electrolyte composition, 0.5 PVdF: 1 EC: 1 PC: 0.7 MgTf (by weight) showed a room temperature ionic conductivity of 1.97×10^{-3} S cm^{-1}. The graph of ln (σT) vs 1000/T is depicted in Fig.1. It shows two features namely,

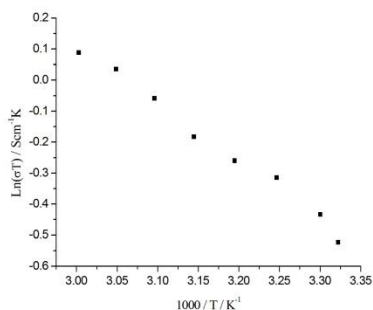i. conductivity increases with temperature

Fig. 1 Variation of conductivity with
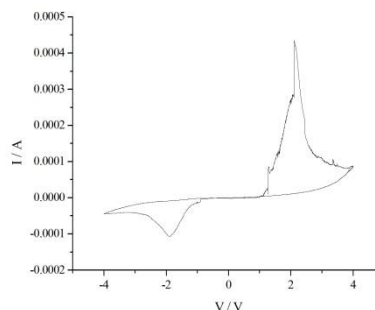
inverse temperature

Fig. 2 Cyclic Voltammogram obtained with Mg

electrodes

ii. temperature dependence of ionic conductivity shows non-linear behavior that follow the Vogel-Tamman-Fulcher (VTF) equation as given in below.

$$\sigma = AT^{-1/2} \exp(-E_a / k(T - T_0))$$

where *A* is a constant, E_a is the activation energy for conduction, k is the Boltzmann constant, T0 is the equilibrium glass transition temperature and T is the temperature.

These features are observed generally for high viscous electrolytes or for much amorphous polymeric systems. The increase in conductivity with temperature has been reported as due to a hopping mechanism between coordinating sites, local structural relaxations and polymer segmental motions (Rajendran et al 2006).

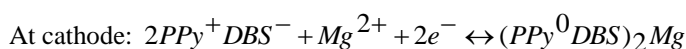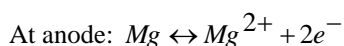Cyclic voltammogram in Fig. 2 has one anodic peak at 2.0 V and a cathodic peak at -1.9 V. They evidenced the fact that mobile species in this electrolyte is Mg ions. The two peaks correspond to the reaction

$$Mg \leftrightarrow Mg^{2+} + 2e^-$$

This is related to reversible plating (reduction) and stripping (oxidation) of Mg ions (Kumar et al 2010). Anodic peak is appearing for stripping and cathodic peak is appearing for plating. Even the peak currents associated with anodic and cathodic peaks are not equal in magnitude, the voltammogram qualitatively suggests that reduction and oxidation processes are taking place in the system.

Average open circuit potential of the cell in the configuration, Mg / GPE / PPy : DBS$^-$ was 1.6 V. Following cathodic and anodic reactions can be suggested as taking place during charging and discharging.

At anode: $Mg \leftrightarrow Mg^{2+} + 2e^-$

At cathode: $2PPy^+DBS^- + Mg^{2+} + 2e^- \leftrightarrow (PPy^0DBS)_2 Mg$

Conclusions

GPE of the composition, 0.5 PVdF: 1 EC: 1 PC: 0.7 MgTf (by weight) has a room temperature ionic conductivity of 1.97×10^{-3} S cm^{-1} which is very convenient to be used for ambient temperature applications. Cyclic voltammetry study shows that Mg ions are mobile in the electrolyte. Cells of the configuration, Mg / GPE / PPy : DBS are suitable to be used for low power requirements.

Acknowledgement

References

Osman, Z., Samin, S.M., Othaman, L. and Isa K.B.M. (2012) Ionic transport in PMMA – NaCF$_3$SO$_3$ gel polymer electrolyte, *Advanced Materials Research* 545 : 259-263

Kumar, G.G., Sampath, S. (2003) Electrochemical characterization of poly(vinylidenefluoride)-zinc triflate electrolyte and its application in solid state zinc batteries, *Solid State Ionics* 160 : 289-300

Tripathi S.K., Jain, A., Gupta, A. and Kumari, M. (2013) Studies on redox supercapacitor using electrochemically synthesized polypyrrole as electrode material using blend gel polymer electrolyte, *Indian Journal of Pure and Applied Physics*, 51 : 315-319

Wu, T.Y., Li W.B., Chou, C.F., Liao, J.W., Chen, H.R., Tseng, C.G. (2012) Study of PMMA based gel polymer electrolytes for electrochromic devices, *International Journal of Electrochemical Science* 8 : 10720-10732

Pandey, G.P., Agrawal, R.C. and Hashmi, S.A.(2011) Performance studies on composite gel polymer electrolytes for rechargeable magnesium battery applications, *Journal of Physics, Chemistry of solids* 72 : 1408-1413

Perera, K.S., Dissanayake M.A.K.L., Skaarup. S., West, K. (2008) Application of polyacrylonitrile based polymer electrolytes in rechargeable lithium batteries, *Journal of Solid State Electrochemistry* 12 : 873-877

Rajendran, S., Sivakumar, P., Babu, R.S. (2006) Investigation of poly(vinylidene fluoride) based gel polymer electrolytes, *Bulletin Materials Science* 29/7 : 673-678

Kumar, D. and Hashmi, S.A. (2010) Ionic liquid based sodium ion conducting gel polymer electrolytes, *Solid State Ionics* 181 : 416-423

INVESTIGATION OF THE EFFECTIVENESS OF UPPARU SALT BARRAGE IN JAFFNA PENINSULA (3rd Stage)

N.Rupathasan[*] and D.T.Udagedara
Uva Wellassa University Badulla, Sri Lanka

D.T.Jayawardhane
Department of Forestry and Environmental Sciences, Faculty of Applied Science, University of Sri Jayewardenepura, Nugegoda, Sri Lanka

Introduction

The Jaffna Peninsula is located in the northern Sri Lanka. The total area of the Jaffna Peninsula is 1036 km^2 and demarcated three internal lagoons such as Thondamanaru, Upparu and Valukiaru. The first two lagoons comprise of an area of 77.6 km^2 and 25.9 km^2. They are connected to the sea and drain an area of 518 km^2. Majority of the local community of the area is depending on agriculture and fishing.
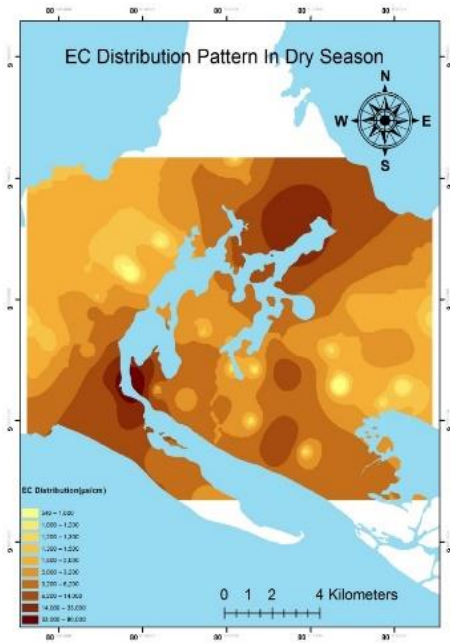
Groundwater is the main source for people in Jaffna Peninsula for domestic and agricultural activities. According to the field observations even people having their own wells, majority of them are affected by salt water intrusions. Therefore, they depend on the common water supply given by the government for drinking purposes, whereas some people still depend on groundwater sources. Recently, barrage was constructed as a salt water exclusion bund to convert the salt water in lagoon Upparu to fresh water lake. This is expected to improve available water resources of the peninsula, both in recharging the underground storage (Sukanya, 2012). This research is focus of the area from the fringe of the lagoon into the land extending around 2 km. Major aim of the research is to evaluate the effectiveness of the barrage by delineating the salt water intrusion pattern especially in the west and northwest areas of the lagoon.
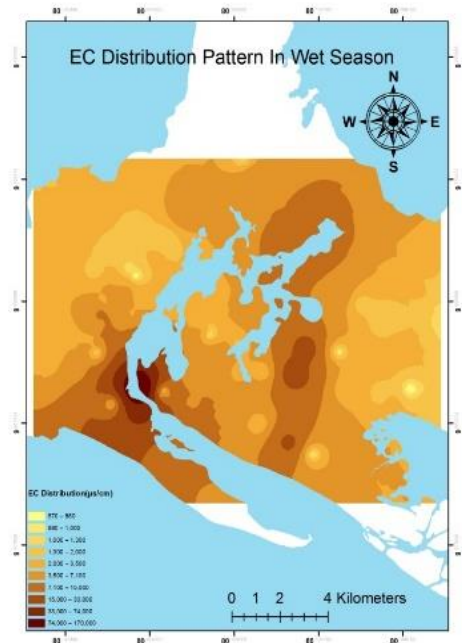
Methodology

Existing aquifer types, geology and topography were studied with the help of available resources and monitoring was done in the area. Wells were selected in a circle to the fringe of Upparu lagoon. The areas coming under study are parts of Nallur, Kopay and Chavakachcheri divisional secretariat divisions. Electrical conductivity (EC) of the groundwater was measured during wet and dry seasons. The wells in which EC show a sudden change was selected for further chemical analysis (sodium and chloride). In addition, both wet and dry season sixty eight (68) shallow well samples were selected for sampling. Water samples were collected in PETF bottles, acidified and capped tightly. Water samples were analyzed for Na using Varian Atomic Absorption Spectrometer (AAS 240 series) facility available at the Uva Wellassa University. Chloride was measured with argentometric method. Spatial distribution of the chemical & physical parameters in the groundwater was interpolated using Inverse Distance Weighted method available in Arc GIS 9.3 software.

Results and Discussion

Results of this study show that EC values for groundwater in the study areas varies between 574 μS/cm and 23,470 μS/cm in wet seasons and between 544 μS/cm and 22,810 μS/cm in dry seasons. Element chloride values range between 449.8mg/L and 7,197.7 mg/L in wet seasons and between 949.7 mg/L and 4,098.7 mg/L in dry seasons. Sodium values vary in between 38.3 mg/L and 802.9 mg/L in wet seasons and between 26.7 mg/L and 648.4mg/L in dry seasons.

(b) - EC

In general, salinity of water depends on the chloride and sodium concentrations in the water. They are the factors controlling the salinity and thickness of fresh water lenses available in the area before and after the inter-monsoon and north-east monsoon rains. Further, due to rapid extraction of groundwater leading to mixing of the saline water with freshwater through the fresh water and saline water interface can be recognized from present study. In addition, changing low and high tides of the lagoons, wrong practice of fertilizer on cultivated lands, geological and structural conditions of the basement and already deposited salt may be the other controlling factors of the salinity of groundwater in the area.

Conclusions

Results obtain from present study indicate that the salinity of groundwater is not only depends on the seawater intrusions. However, if the barrage is working properly groundwater in the fringe of the lagoon can be expected to change in to fresh water. Which can be used to cultivate 11,000 acres of agriculture land effectively.

References

Sukanya B, Investigation of the Effectiveness of Salt Barrage in Jaffna Peninsula, 2012

Shanmugarajah, K., 1993.Water resources development Jaffna Peninsula.Wild & Woolley Pty.Ltd., Australia

Balendran, V.S., Srimanne,C.H.I.& Arumugam,S. 1968.Ground Water Resources of the Jaffna Peninsula. Water Resources Board, Colombo

Panabokke, C.R, and A.P.G.R.L. Perera., 2005. *Groundwater resources of Sri Lanka*. Water Resources Board, Colombo, Sri Lanka

Cu₂O Quantum Dots (QDs) Sensitized Cu/p-CuI Photo-electrode for H₂ Generation through Efficient Water Splitting

R. D. A. A. Rajapaksha, C. A. N. Fernando

Nano-technology Research Laboratory, Department of Electronics, Faculty of Applied Sciences, Wayamba University of Sri Lanka, Kuliyapitiya, Sri Lanka.
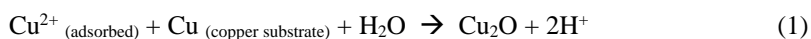
and

S. N. T. De Silva

Department of Biotechnology, Faculty of Agriculture & plantation management, Wayamba University of Sri Lanka, Makandura, Sri Lanka.

Introduction

Water splitting by sunlight to generate hydrogen and oxygen is a fascinating way of energy production. Metal oxides such as Cu_2O, TiO_2, ZnO and WO_3 with various morphologies have been investigated for water splitting (Fujishima & Honda, 1972). However, most of these metal oxides have large band gaps, which limit the light absorption in the visible region and hence the overall efficiency of the process. To achieve a better photoelectrochemical response with these materials, an extensive research has been done on adding nanostructures (Feng et al., 2008; Wu & Yu, 2004). One possibility is the use of semiconductor nanocrystals (3D nanostructure), known as quantum dots (QDs), as an alternative to this problem (Adachi et al., 2004). In this research study, H_2 generation at QDs is presented for the first time efficiently. Energy level positions were used to confirm the QD sensitization process associated at Cu/p-CuI/QD electrolyte interface.

Methodology

Cu/p-CuI photoelectrodes were immersed in $CuSO_4$ (10^{-3}M) solution and boiled until the formation of Cu_2O QDs on p-CuI nano-particles at Cu/p-CuI. Variation in boiling time produce various sizes of Cu_2O QD on Cu/p-CuI electrode and colour variation according to the boiling time is shown in Fig.1 (b-f). Table 1 shows the variation of the extent of Cu_2O QD produced on the Cu/CuI photoelectrode by weight with boiling time in $CuSO_4$ solution. The mechanism of the formation of QDs on the p-CuI particles may be presented from the following reaction.

$$Cu^{2+}_{(adsorbed)} + Cu_{(copper\ substrate)} + H_2O\ \rightarrow\ Cu_2O + 2H^+ \qquad (1)$$

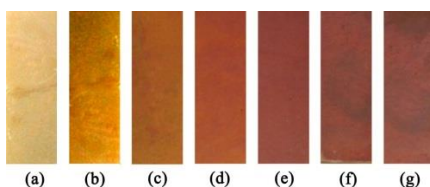The amount of produced H_2 gas was estimated from gas chromatography (Shimadzu GC-2014).

Figure 1: (a) Cu/p-CuI cell- 5min immersing time in $KI/CuSO_4$ solution. Figure (b), (c), (d), (e), (f) and (g) are shown in Table 1.

Table 1: Cu_2O QD amount formed by boiling Cu/CuI samples in a $CuSO_4$ solution.

Electrode	Boiling Time (min)	Cu_2O Weight (μg)
(b)	5	0.4
(c)	10	2.2
(d)	15	3.1
(e)	20	3.9
(f)	30	8.2
(g)	45	9.6

Results and Discussion

Fig.3 shows the variation of H_2 evolution GC profiles with time for samples exhibited in Fig.1(b)-(g) in the presence of 0.025M Na_2SO_4 electrolyte buffered at a pH of 5.2 under visible light irradiation. It should be mentioned that Cu/p-CuI photoelectrodes did not produce any considerable amounts of H_2 under visible light irradiation. The highest H_2 generation exhibited for the samples prepared by boiling Cu/p-CuI photoelectrodes in $CuSO_4$ (10^{-2}M) solution for 20min (sample-(e)). After the saturation of H_2 evolution, H_2 bubbles were accumulated on Cu/p-CuI/QD photoelectrode without showing any photo degradation of the photoelectrodes. During the H_2 evolution process a remarkable photocurrent was observed under the illumination confirming that the H_2 generation caused only from the photogenerated electrons. The mechanism of the H_2 generation can be explained from the following reactions.

$$QD \quad \rightarrow \quad QD^* \tag{2}$$

$$QD^* \rightarrow \quad QD^- + h \, (VB \, p\text{-}CuI) \tag{3}$$

$$QD^- + H^+ \rightarrow \frac{1}{2} H_2 + QD \tag{4}$$

The CB position of the QD may be more negative according the onset potentials obtained from the V-I characteristics curve and the energy level diagram as shown in Fig.2. So that QD^* produced photogenerated electrons can transfer to H^+/H_2 redox level efficiently to generate H_2 under visible light.
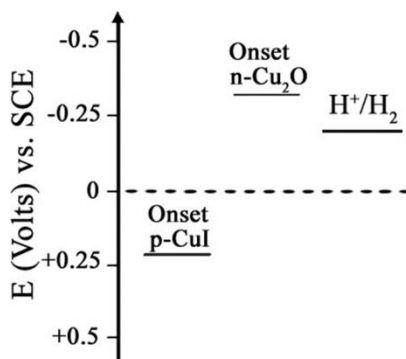

Figure 2: Estimated band positions of p-CuI, n-Cu_2O and H^+/H_2 redox levels with respect to Ag/AgCl.
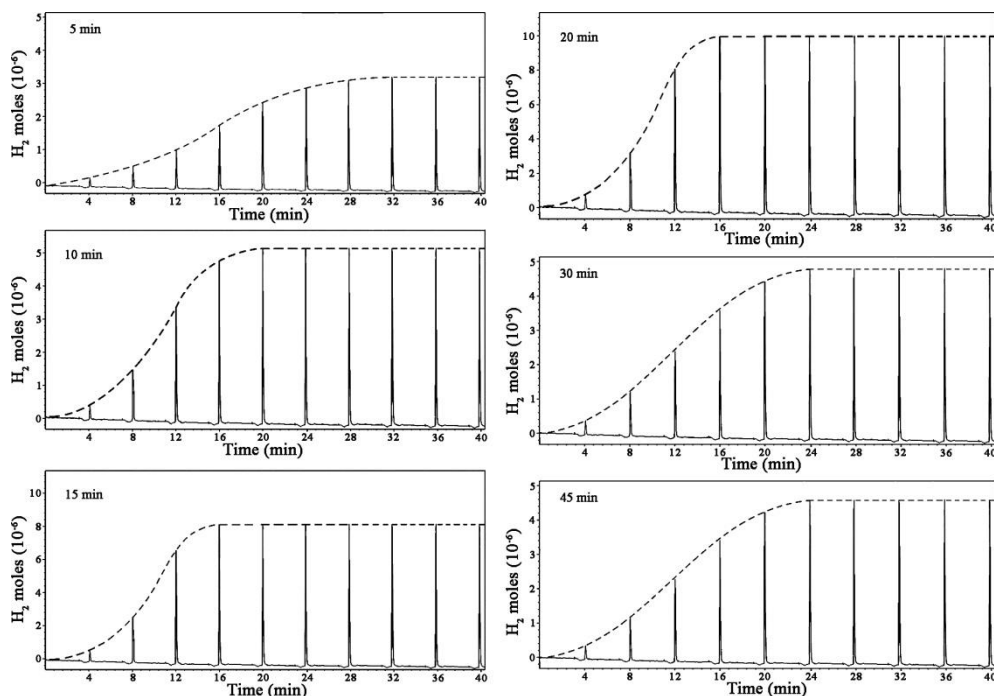
Figure 3: The variation of H_2 production with time measured by gas chromatography for various samples at maximum H_2 production voltage vs. Ag/Agcl in the presence of 0.025M Na_2SO_4.

Conclusions

p-CuI was sensitized by Cu_2O quantum dots for the first time in a photoelectrochemical cell at low cost and easy fabrication processes on a well cleaned commercially available copper sheets. When the size of the QD increased, a photocurrent quantum efficiency enhancement was observed. Any chemical dissolution of p-CuI or Cu_2O QDs not significant after long time irradiation profiles. H_2 generation was presented with the different sizes of the QDs from photogenerated carriers at Cu/pCuI/QD-electrolyte interface.

Acknowledgement

References

Adachi, M., Murata, Y., Takao, J., Jiu, J. T., Sakamoto, M., Wang, F. J., 2004. *J. Am. Chem. Soc.*, 126, pp.14943-49.

Feng, X., Shankar, K., Varghese, O.K., Paulose, M., Latempa, T.J., Grimes, C. A., 2008. *Nano Lett. 8 (2008) 3781e3786.*, 8, pp.3781-86.

Fujishima, A., Honda, K.., 1972. *Nature*, 238, pp.37.

Wu, J.J., Yu, C. C., 2004, *J. Phys. Chem. B* 108 pp.3377-3379.

Enhancement of solubility of Eppawala Rock Phosphate through Bioleaching

T.C. Senevirathna*, C.M. Peries and J.T. Cooray
Uva Wellassa University, Badulla, Sri Lanka

Introduction

Phosphorus (P) plays an indispensable biochemical role in photosynthesis, respiration, cell division and several other processes in the living plant (Grover, 2003). An inadequate supply of phosphorus in the early stages of plant growth reduces most of these physiological functions and ultimately reduces the crop productivity. Therefore, external applications of P fertilizers is necessary in terms of better crop production. Locally available P resources like Eppawala Rock Phosphate (ERP) deposits are now highly concerned due to the environmental effects and the high cost of imported P fertilizers. However, the ERP is considered as less applicable local P resource for short term cultivations due to the low solubility. Although chemical treatments are highly available to solubilize ERP, the cost of application is fairly high. In that sense, the inoculation of naturally existing P-solubilizing microorganisms is considered as a promising technique to solubilize P sources due to the low application cost and giving a thrust to economic development without disturbing ecological balance (Reyes *et al*., 2002). Thus, this study was focused on screening the P solubilizing microorganisms (PSM) from ERP deposit and apply them to enhance the solubility of ERP and High-Grade Eppawala Rock Phosphate (HERP).

Methodology

Powdered Rock Phosphate samples were collected from the rock phosphate stockpile of phosphate mine of Lanka Phosphate Limited, Eppawala. Microbial isolation were performed from the obtained Phosphate samples using standard microbiological techniques. Isolated microbial strains were inoculated on PVK medium, a selective medium to screen PSM. Thereafter, screened microbial strains were inoculated in PVK broth media containing either ERP or HERP separately. P content in each sample was determined using UV spectrophotometric method after 1st, 2nd, 4th and 7th days of inoculation.

Result and Discussion

Four bacterial strains and four fungal strains were initially isolated using the rock phosphate samples obtained from phosphate mine of Lanka Phosphate Limited, Eppawala, Sri Lanka. Out of them, two bacterial strains (B1 and B2) were selected as potential phosphate solubilizers based on the development of clear halo zone on PVK agar medium due to the P solubilization in the surrounding medium (Fig. 1 a and b).

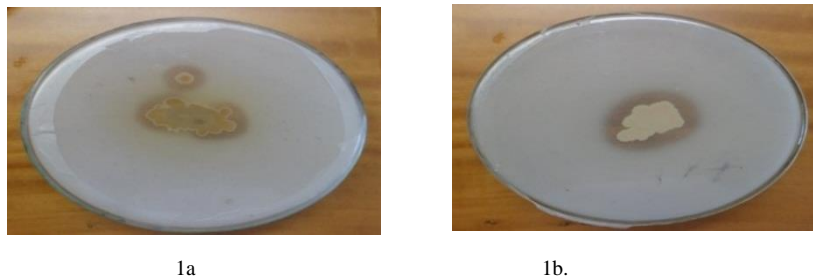1a   1b.

Figure 1- Different bacterial strains exhibiting halo zones on PVK medium due to the P solubilization. (a)- Halo zone observed due to the bacterial strain B1. (b)- Halo zone observed due to the bacterial strain B2.

It has been reported that the PVK medium can be used to isolate PSM based on the formation of clear halo zone on Calcium Triphosphate of PVK medium due to the organic acid production by PSM (Sharma, 2005).
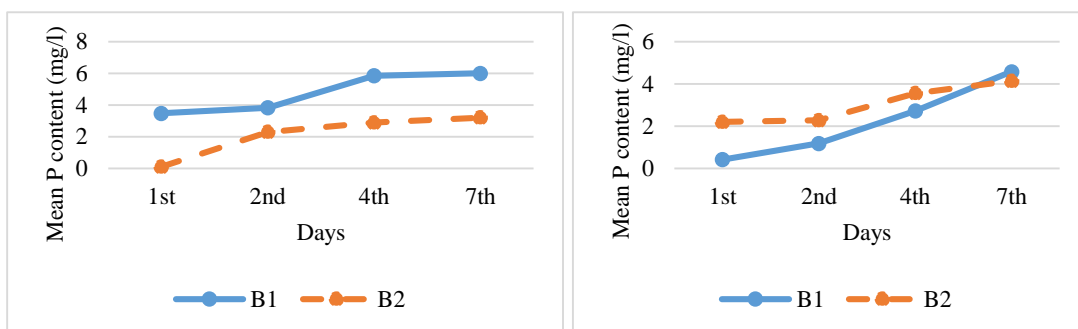

Figure 2- The effect of the bacterial strains on P solubilization of different Phosphate sources. (a)- The effect of bacterial strains on HERP. (b)- The effect of bacterial strains on ERP. Phosphate concentration was measured different days with in a week.

According to the statistical analysis, a significant correlation was observed between the type of the phosphate and the bacteria ($P< 0.05$). Further, the pH of the media after the bacterial inoculation were changed to the acidic range (pH 3-5) after seven days. It has been reported that the PSM solubilize soil P by the production of low molecular weight organic acids such as gluconic and keto gluconic acids, thereby reducing the pH. Furthermore, these PSM have the capability of tolerating harsh conditions like high acidic environments (Nautiyal *et al*, 2000).

Bacterial strain B1 showed higher P solubilizing ability on HERP compared to the bacterial strain B2 (Fig. 2a). It was observed that the P solubilization rate in both bacterial types was enhanced up to the fourth day and after that the rate become constant (Fig. 2a). This might be due to the limitation of nutrient and accumulation of metabolites with the time in the growth media. Further, bacterial strain B1 showed lower P solubilizing effect on ERP phosphate type compared to the strain B2. It has been reported that ERP contains great amount of impurities compared to HERP (Hewawasam, 2013). Therefore, these impurities might have an effect on the efficacy of B1 activity at the initial growth period. However, it was clearly observed that the P solubilizing rate

by the bacterial strain B1 on ERP was extremely enhanced after first day and the B1 strain showed the highest solubilized P content compared to the strain B2 at the seventh day (Fig. 2b).

Conclusions

It can be concluded that the bacterial strains B1 and B2 have positive effects on solubilizing ERP and HERP sources. Bacterial strain B1 has higher efficiency on solubilizing HERP. The effect of B1 and B2 on P solubilizing should be further evaluated at the field conditions.

Acknowledgement

Laboratory facilities provided by the Uva Wellassa University are acknowledged.

References

Grover, R. (2003). Rock phosphate and phosphate solubilizing microbes as a source of nutrients for crops. MSc. Thesis. Thapar Institute of Engineering and Technology, Patiala.

Hewawasam, T. (2013). Tropical weathering of apatite-Bearing Rocks of Sri Lanka: major element behaviour and mineralogical changes. Journal of Geological Society of Sri Lanka. 15, 31-46.

Nautiyal, C. S., Bhadauria, S., Kumar, P., Lal, H., Mondal, R., and Verma, D. (2000). Stress induced phosphate solubilization in bacteria isolated from alkaline soils. FEMS Microbiology Letters. 182, 291-296.

Reyes, I., Bernier, L. and Antoun, H. (2002). Rock phosphate solubilization and colonization of maize rhizosphere by wild and genetically modified strains of *Penicilliumrugulosum*. Microbial Ecology. 44, 39-48.

Sharma, S., Kumar, V. and Tripathi, R.B. (2011). Isolation of Phosphate Solubilizing Microorganisms (PSMs) from soil. J. Microbiol. Biotech. Res. 1(2), 90-95.

Purification of Surface Graphite from Passyala, Sri Lanka

R.M.U.M. Somarathna[1]*, N.W.B. Balasooriya[2]

[1] Uva Wellassa University, Passara Road, Badulla, Sri Lanka
[2] Faculty of Applied Sciences, South Eastern University of Sri Lanka, Sammanthurai, Sri Lanka

Introduction

Flake graphite occurs as isolated, flat plate-like particles disseminated in lenses or pockets in metamorphic rocks. Less frequently it occurs in massive accumulations in veins. This is the geologically most common variety of natural graphite. Surface graphite (flake graphite) deposits occur at South Western region of Sri Lanka. There were large number of shallow pits in Sri Lanka had historically been sunk in to the weathered rock or top soil and believed more than 2500 graphite pits and mines were located in the west and central highlands. Graphite exploration from Matugama, Warakapola, Passyala and Deniyaya are in progress as new sites. Even though there are various studies on Sri Lankan vein graphite, limited attention was drawn to study the distribution, chemistry, origin and geology setting of surface graphite deposits in Sri Lanka. (Wijayananda N.P.,1987).Froth Flotation is versatile mineral processing technique, that utilizes the difference in surface properties of the valuable minerals and the unwanted gangue minerals to achieve specific separations from complex ores. Graphite have non-polar surface that do not readily attach to the water dipoles. Therefore in the separation graphite can be effectively collected into the froth. (Wills B.A.,2006). considering the chemical purification, recent studies on flake graphite with alkali roasting proven that the purity can be upgraded over 95%. (Lu, X.J., *et al*,2002) Present research was aimed to study the purification of Sri Lankan flake graphite by using both chemical and physical purification techniques.

Materials and methodology

Initially collected samples were crushed into chips and prepared powder samples (<250 μm) for both sample no-01(taken from Wawehena mine) and 02 (taken for Kaluaggala mine). 200g from each samples were taken into froth flotation. Separated froth was washed to remove the effect of phenol and dried at 60 ^{0}C for 24 hours.

3g from each graphite sample was take into alkali roasting, mixed with 10,20,30,40,50,60 vol. % NaOH (solid: liquid, 1:2) separately and roasted at 250 ^{0}C under air for one hour. The roasted sample was acid-leached in 10 vol. % H_2SO_4 and filtered. The residue was washed to neutral and vacuum dried at 100 ^{0}C for 15 hours . (Lu, X.J., *et al*,2002).Carbon percentage of graphite was determined according to ASTM - 561 and weighing the residues. Both initial and froth floated graphite matrix was characterized by Fourier Transform infrared (FTIR) spectrophotometer in 500 - 4000 cm-1 region (Nicolet 6700). The electrical characterization was performed on the dense graphite pellets by four probe d.c. conductivity in air.

Results and discussion

Table - 4.1 shows the measured carbon content for both sample 01 and 02, before and after froth flotation. Forth flotation was able to achieve averagely 35% purity enhancement for the collected

flake graphite samples. Therefore it clearly evident that the forth flotation technique is much effective as an initial purification technique before moving to the chemical or any other purification method.

Table 4.1: Carbon Percentage of both sample 01 and 02, before and after froth flotation

Sample No	Initial purity	After froth flotation	Effective Enhancement from froth flotation
No -01	27.3%	60.0%	32.7%
No -02	29.6%	67.4%	37.8%

Figure - 1 shown comparative illustration of NaOH concentration Vs carbon percentage of sample no-1 (left) and sample no-02 (right) respectively. Sample no-01 could able to reach it maximum purity value 95.64% with 40% of NaOH but there is no gradual increment in carbon percentage with the increment of NaOH concentration. Though in sample no-02 there is an increment of purity enhancement and it seems to be matured after 40 % NaOH concentration. It marked the maximum purity 97.98% at 50% of NaOH concentration. Further increment of the NaOH concentration may not be significant.
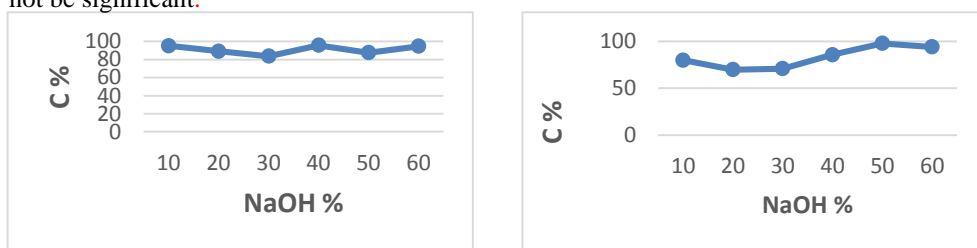

Figure - 1: Effect of NaOH concentration on purity enhancement for sample no 01(left) and sample no-02(right), roasting at 250 ^{0}C
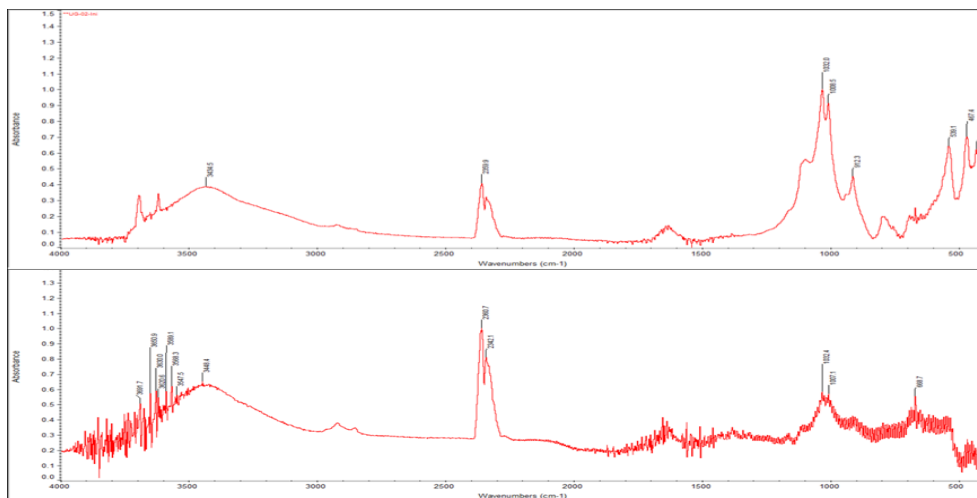

Figure – 2 - Fourier transform infrared spectroscopy-FTIR (KBr Pellets, Absorbance mode) curves for the sample no-01 (A) and sample no-02 (B) after froth flotation.

Figure-2 provide a comparative illustration of FTIR analysis for froth floated samples (for sample no-01 and 02). The broad band between 3500 and 3100 cm^{-1} and the band at~ 1620 cm^{-1} are attributed to the bending mode of the molecular water. The doublet band at~2360 cm^{-1} and 2342 cm^{-1} can be assigned as a characteristic band for graphite. When both sample 01 and 02 were in initial stage the mentioned characteristic band was suppressed. Though the FTIR curve after froth flotation evident significant presence of that particular band with a better absorption

The D.C. electrical conductivity details of graphite samples after froth flotation and purification are given in Table-2. Electrical conductivity of raw graphite samples was not measured because they have low carbon percentage and contained various impurities which can affect the electrical conductivity more than that of graphite in the sample such as weathered laterite soil.

Table – 02 D.C. electrical conductivity of graphite samples after froth flotation and purification.

Sample no	Initial purity	Conductivity after froth flotation / Scm^{-1}	Enhanced purity	Used NaOH concentration	Final conductivity / Scm^{-1}
01	27.3%	38.28	95.64%	40%	9.41
02	29.6%	16.68	97.98%	50%	8.28

Electrical conductivity values after the froth flotation were 38.28 Scm-1 for sample 01 and 16.68 Scm-1 for sample 02. These values are relatively high for graphite. These samples still contain significant amount of impurities which may be the reason for these high electrical conductivity values. Finally electrical conductivity values are relatively lower and vary around 9 Scm-1. This clearly indicate that the alkali roasting could able remove the impurities which influenced the electrical conductivity and enhance the performance of flake graphite.

Conclusion

Carbon content analysis results shown that froth flotation is very much effective for the purity enhancement of flake graphite. As a chemical purification alkali roasting shown a profound effect on purity enhancement. Samples with lower initial purity shown good enhancement at 40-50 % NaOH concentration. Therefore it can be conclude that it is possible to purify low grade surface graphite (flake graphite) to obtain high purity graphite (<97% C) using both identified chemical and physical methods.

References

Wijayananda N.P. (1987). <u>The Graphite Industry Sri Lanka</u>. State Mining & Mineral Development Corporation, Sri Lanka.

Wills, B.A., Napier-Munn T., (2006). <u>Mineral Processing Technology - An Introduction to the Practical Aspects of Ore Treatment and Mineral Recovery.</u>7th edition, Elsevier Science & Technology Books.

Lu, X.J., Forssberg, E.,(2002). <u>Preparation of high-purity and low-sulphur graphite from Woxna fine graphite concentrate by alkali roasting,</u> Minerals Engineering, Vol. 15, p.755–757.

Purification of Meetiyagoda Kaolin for boron free glaze manufacturing

M.H.S. Hussain[*], and J.T.Cooray
Department of Science and Technology, Uva Wellassa University, Badulla, Sri Lanka.

S. Medawela
Lanka Tiles (PLC), Jaltara, Ranal, Sri Lanka.

Introduction

A tile is a manufactured piece of hard-wearing material such as ceramic, stone, metal, or even glass for covering of roofs, floors, walls, or other objects. Tiles are often made from ceramic with a hard glaze finish. But sometimes with other materials such as glass, marble, granite and slate are also used to produce tiles. Among them, floor tiles are commonly made of ceramic, porcelain and stones due to their attractiveness, durability, and easiness to clean. The main components of a tile are tile body, glaze layer, and printed layer. The raw materials used to form a tile consist of clay minerals, quartz, feldspar which is used to lower the firing temperature and chemical additives required for the shaping process. Tile decoration is mainly depending on the glaze layer. Sodium feldspar, potassium feldspar, quartz, wollastanite and kaolinite are abundantly used materials in glaze production. Even through Sri Lanka contains most of the above raw materials; at present all required glaze materials as imported to the country due to the cost, lack of technology and some quality problems of raw materials. So this research aims to manufacture a low cost glaze medium mainly using local mineral materials and few imported materials.

Methodology

The current study was carried out at Uva Wellassa University, Badulla, Sri Lanka and Lanka Tiles PLC, Jaltara, Sri Lanka. First, the raw materials were purified to make frit and glaze. The acid leach process was carried out for purification of kaolin and the magnetic process was carried out feldspar, wollastanite and quartz. The clay sample selected for investigation was kaolinite clay obtained from Meetiyagoda area. Then the clay sample was ground using a laboratory ball mill to -149 μm (100 meshes). The ground clay sample was placed on the sieve, and then mechanically shacken for 5 min. The oversize was further grounded followed by sieving with the same sieve. The procedures were repeated till the entire clay sample passed through the sieve. After that ground clay sample passing 100 mesh was subjected to calcination. The sample was heated at 600ºC for 1 h (using a muffle furnace with a maximum temperature of 1200 ºC) to activate the clay before acid treatment (Al-Zaharani and Abdulmajid, 2009). Calcineated clay sample passing 100 mesh were leached using 3M hydrochloric acid for different periods of time (10-150 min) and at different leaching temperatures (25ºC to boiling temperature) using a constant temperature shaking water bath at a fixed shaking rate of 160 cycles/min and using boiling under reflux (Hulbert and Huff, 1970). At the end of leaching, the resulted slurry was filtered to separate undissolved materials and, washed in distilled water. The filtrate and washings were continued

until ions were removed in the sample. The resulting sample was dried for 24 h in Laboratory oven. Likewise the feldspar and wollastanite were purified by magnets. The purity and quality of leached kaolinite were tested using common base (CS 100) in tile industry. After that the frit was made using 80g of sodium tetraborate pentahydrate ($Na_2B_4O_7.10H_2O$), 100g quartz, 160g of kaolin, 40g of wollastonite, 20g of zirconium silicate and 5g sodium chloride. The raw material was mixed in a pot mill. Water was added slowly step by step until the mixture forms in to a crumb. The crumb was heated at 100^0C until it was completely dry. Then the dried product was transferred to porcelain cups and it was placed in a laboratory muffle kiln. The kiln was heated at a rate of 4^0C per minute up to a 1050^0C and kept at same temperature for 90 minutes (Simon et al, 2007). The furnace was switched off and the crucible was allowed to cool down to ambient temperature in the furnace. The product was removed, wrapped in a plastic film hammered to break in to small pieces. Then the base formula was generated by using it. Glass formation and formulation mechanisms (fluxes, vitrifying agent, opecifier), thermal expansion of the materials and melting point (softening temperature) were considered for base making. The materials in the base thermal expansion were adjusted according to frit thermal expansion. Frit (30g), kaolin (8g), sodium feldspar (30g), wollastanite (32g), zirconium silicate (10g), aluminium oxide (2.5g), zinc oxide(1.5g), C.M.C (0.2g) and S.T.P.P (0.2g) were added to the base formula and it was grind with 100 ml water in pot mill for about 20 minutes. Resulted base medium was sieved using a 100 μm sieve and it was sprayed by spray gun on to engobe green tile. Base density and base viscosity was measured before spraying. Based tile was fired in the kiln. Finally fired tile surface properties, thermal shock, abrasion, strain, cracking and acid resistance were checked to ensure the quality.

Results and Discussion

Leach kaolin base is whiter than the reference base which is used to compare. But there were pin holes on glaze surface which may have caused by organic materials in kaolin. Pin holes are considered as a defect in the tile body. The challenge of reducing pin holes can be achieved by changing firing zone, but it cannot be adjust for one tile. Therefore, pin holes were reduced by making rougher the tile surface by adding alumina in to the base. After adding alumina, the result shows that it can use for glaze making.

Prepared frit is opaque and I has matt surface when it was fired with the 90% of frit and 10% kaolin. This frit generates a slightly rough surface compared to the other commercially available verities as this cooled under slow cooling environment and there, it produces a crystalline surface instead of a vitreous surface. Even though fast cooling is essential in making frit, it is   impossible to achieve that with a laboratory muffle kiln. Therefore this frit was used in production of base by adjusting other raw materials.

Prepared base is white in colour and has a glossy surface and also fulfil the all quality tests.

- **Tile code – Sample**
- **Ceramic Body – White**
- **Tile Size – 300 X 300 mm**

  Table 1: Technical characteristics of new tile

	CHARACTERISTICS	RESULT
1	STAIN RESISTANCE	PASS

2	ACID RESISTANCE	PASS	
3	ALKALI RESISTANCE	PASS	
4	PEI CLASS	3	
5	SLIP RESISTANCE (PENDULUM TEST)	~~WET~~	DRY
		~~FAIL~~	PASS
6	THERMAL SHOCK RESISTANCE	PASS	
7	CRAZING ABILITY	PASS	
8	CLEANING ABILITY	VERY EASY EASY ~~DIFFICULT TO CLEAN~~	
9	CUTTING ABILITY	YES	

Table 2: Dimensional characteristics of new tile

Product tile Warpage (mm)						Centre curvature (mm)		
Tile no	1	2	3	4	Range	1	2	Range
01	-0.01	0.22	-0.11	0.30	0.44	-0.11	-0.04	-0.03
02	0.12	0.27	0.25	0.04	0.21	-0.05	-0.14	-0.09
03	0.05	0.28	-0.15	0.11	0.43	0.29	0.36	0.07

Conclusion

Main objective of this research is to prepare boron free glaze from purification of Meetiyagoda kaolin and other local minerals. Purification was successfully achieved by hydrochloric acid leaching of kaolin and removal of iron using a magnet in feldspar, quartz and wollastanite. Using standard methods these materials were formed in to a suitable base material to be used in glaze, which is satisfy all quality test.

Pin holes were appeared due to presence of organic materials, by adding aluminium oxide in to the base those can be reduced.

Cost of leaching Meetiyagoda kaolin is high; therefore overall cost of the base was also high. Because of that the imported kaolin (*BO kaolin*) was used in the process and the resulted also shows the same quality.

References

Al-Zahrani, A.A. Abdulmajid, M.H. (2009). Extraction of alumina from local clays by hydrochloric acid process. JKAU:Eng.Sci, vol.20 No.2, 29-41

Hulbert, S.F. Huff, D.E. (1970). Kinetic of alumina removal from a calcined kaolin with nitric, sulphuric and hydrochloric acids. Clay Minerals 8,337-345

Simon Geyson Cook, Cercos Miguel Joaquin Galindo, Glaze compositions, WO 2007148101 A1, 2007

Groundwater Contamination around in Paddy Terrace in Badulla; special focus on nutrients and tracer element mobility

W.N.C.Wijenayaka[*]
Uva Wellassa University, Badulla, Sri Lanka

D.T.Jayawardhana
University of Sri Jayawardanapura, Sri Lanka

Introduction

Groundwater is the water located beneath the earth's surface in soil pore spaces and in the fractures of rock formations[4]. Pollution of groundwater due to contaminated soil and fertilizer/pesticide is hurt animals, plants or humans and it may cause serious health problems, such as, hepatitis, blue baby syndrome, kidney disease, *etc* (Dissanayake *et al*., 1984).

Paddy terrace is artificial replacement of nutrients in damage land. Due to erosion, nutrients were removed from top soil. Therefore, farmers are needed to apply especially N, P, and K fertilizer in artificial replacement. As a result of artificial nutrients added, groundwater can be highly contaminated around paddy terraces. Previous researchers investigated the sediment and nutrient (N, P, and K) movement behavior in terraced paddy fields system and groundwater contamination around paddy terraces has not been conducted in Sri Lanka. Thus, this research aims at identifying the excess nutrients and tracer elements with the excess pesticides/fertilizers from terrace paddy farming on groundwater and surface water. Also, it is attempted to identify mobility of them to groundwater and surface water during the different stages of the paddy cultivation.

Materials and methods

A total number of 80 water samples were collected from Rabukpotha area in Badulla, Sri Lanka, at frequent intervals during February to early July 2014, which coincides with the *Maha* season. The sampling was carried out in two stages of the intermediate period. Before and after cultivation two sample sets were collected and sample sets were renamed as A and B, respectively. Eighty water samples were analyzed for 25 chemical parameters (temperature, pH, Eh, turbidity, NO_3^-, PO_4^{3-}, NH_4^+, SO_4^{2-}, CO_3^{2-}, HCO_3^-, F^- Cl^-, Na, K, Mg, Ca, Cu, Pb, Zn, Mn, Fe, Rb, Li, Sr, Cs). Nutrients and tracer elements were measured using titrimetric, spectroscopic methods such as atomic absorption spectrometer and UV/Visible spectrophotometer[1].

Results and Discussions

Measured parameters are summarized in Table 01. pH levels vary in both stages in the eighty water samples. The values were a range from 6.0 to 8.53. The normal recommended pH range for irrigation water is from 6.5 to 8.4 [2]. All the tested wells were within the range irrigation water and there were no influence of cropping system on pH. EC levels were a range from 0.28 mS/cm to 5.72 mS/cm. Some of the wells EC values were increased after cultivation due to the leaching of salt from soil. Fluoride concentration on groundwater is not in detectable level. With the accuracy of instrument, low concentration might not be detected. Data analysis showed that higher Cl⁻, Fe and

Mn concentration was present in groundwater with the usage of fertilizer. Also, after adding fertilizer, some elements (NO_3^-, NH_4^+, Cu and Sr) are present in elevated concentration, except other elements. Those tracer elements and nutrients are leached to shallow wells faster than others.

Table 01: Minimum , maximum and average values of parameter in groundwater

Parameter	Sample Type A (n=40)				Sample Type B (n=40)			
	Min	Max	Mean	Std. Dev.	Min	Max	Mean	Std. Dev.
pH	6.47	8.40	7.50	0.49	6.01	8.53	7.65	0.71
Trubidity (NTU)	0.13	33.70	5.33	6.84	0.14	45.10	3.05	7.34
Conductivity (mS/cm	0.46	2.14	0.86	0.33	0.20	5.72	0.98	1.01
ORP (mV)	-145.00	58.00	-39.20	52.71	-78.00	32.00	-11.73	26.05
Cl^-(mg/L)	1.234	65.980	12.650	13.503	3.999	59.981	16.995	10.705
F^-(mg/L)	0.000	ND	ND		0.000	ND	ND	
NO_3^-(mg/L)	0.229	4.040	0.809	0.901	-0.397	12.505	2.068	2.363
PO_4^{3-}(mg/L)	-0.001	0.001	0.000	0.000	-0.002	0.003	0.000	0.001
NH_4^+(mg/L)	0.064	0.287	0.143	0.055	0.119	0.361	0.168	0.079
Cu (mg/L)	0.003	0.084	0.026	0.017	0.000	0.140	0.020	0.028
Fe (mg/L)	0.000	1.940	0.280	0.403	0.000	1.701	0.107	0.388
Zn (mg/L)	0.002	2.242	0.032	0.384	0.000	0.185	0.020	0.044
Mn (mg/L)	0.000	0.709	0.012	0.151	0.004	0.310	0.021	0.076
Cs (mg/L)	0.895	1.827	1.311	0.233	0.009	1.377	0.460	0.476
Sr (mg/L)	0.001	0.368	0.085	0.065	0.015	0.464	0.108	0.096
Li (mg/L)	0.000	0.008	0.006	0.002	0.002	0.014	0.005	0.004
Rb (mg/L)	0.014	0.177	0.096	0.046	0.007	0.170	0.090	0.041
Na (mg/L)	5.435	30.358	6.129	4.051	4.978	48.375	7.857	10.802
Ca (mg/L)	2.288	26.670	10.571	5.027	2.468	47.408	10.298	11.261
K (mg/L)	1.625	15.963	3.361	2.328	1.655	12.563	5.231	3.733
Mg(mg/L)	0.024	19.220	9.521	3.368	4.170	31.729	7.664	6.552

Ca-Mg-HCO_3 type groundwater facies was presented in study area (Figure 1).
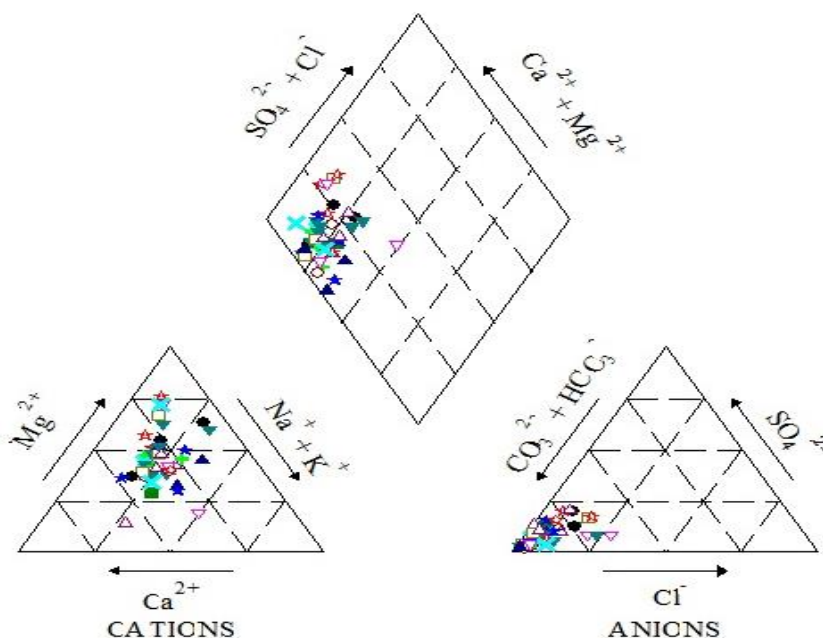
Figure 5: Piper diagram showing the major ions water quality

Conclusions

Some of the elements are (Cl^-, Fe, NO_3^-, Mn, NH_4^+, Zn, Sr) leach to groundwater with highly usage of artificial fertilizer. Samples which are collected from near the paddy terrace present higher nutrients and tracer elements concentration beyond others. There is significant different between before and after cultivation. With the terrace arrangement, tracer elements and nutrients are enriched in low land areas as compared with other areas. The overload of nitrogenous fertilizers to the soil is help to provide elements to soil. But some nitrogenous fertilizers are not subject to immediate leaching. Also phosphorous fertilizer is less subject to leaching, but it loss through surface runoff. Therefore it is difficult to say some elements directly contributed by agrochemicals.

Acknowledgment

The authors are highly thankful to Uva Wellassa University, Badulla for providing necessary laboratory facilities for the research.

References

1) Andrew D. Eaton, Lenore S. Clesceri, Eugene W. Rice, Arnold E.Greenberg, 2005, Standard Methods, 21st edition, Maryland, Port city press, pp 4-85, 4-86, 4-120, 4-121, 4-188, 4-189

2) Ayres, R.S. and D.W. Westcot, 1985. Water quality for agriculture. Irrigation and drainage. Paper No.29. FAO, Rome.

3) Dissanayake, C.B., Weerasooriya, S.V.R. and Senaratne, A. (1984) The distribution of nitrates in the potable waters of Sri Lanka, Aqua No.1, pp. 43-50.

4) Travelogue of an armchair traveler, 2012. World's Largest Terraced Paddy Fields, Yuen Yang, China(13th May 2012)

Use of computational method to identify metal binding sites of chitosan as a tool to investigate the interaction mechanism of chitosan and heavy metals

S.M. De Silva and C.S.K. Rajapakse

Department of Chemistry, Faculty of Science, University of Kelaniya, Sri Lanka

Introduction

A bioadsorbent chitosan; a derivative of chitin polysaccharide composed of randomly distributed β-(1-4)-linked D-glucosamine and N-acetyl-D-glucosamine (Cahyaningrum *et al.,* 2004) was reported by our group to be much effective as a drinking water purification agent as the percent removal of Cd(II), Pb(II) and Cr(VI) from drinking water by chitosan were 94%, 64% and 70% respectively under optimized conditions (De Silva *et al.,* 2014). It is widely known that chitosan can make complexes with certain metal ions as chitosan has different possible binding sites for metals (figure 1). But little attempt has been made to understand the interaction mechanism of chitosan and heavy metals. Hence the aim of this study was to simulate the IR spectrum of chitosan by DFT calculations and to identify the vibrational bands associated with the possible metal binding sites which can be used as a tool to investigate the interaction mechanism of chitosan and heavy metals.

Methodology

All theoretical calculations reported in this study were carried out by use of the Gaussian 09 program package. Although chitosan is a polymer, a trimer shown in figure 01 was used to represent chitosan in all theoretical studies. First the structural parameters of the optimized structure of the chitosan have been obtained using electron density functional theory (DFT) with the Becke–Lee–Yang–Parr functional (B3LYP) and 6-31G (d) basis set employing in a gas phase model. Then the IR spectrum of the chitosan was simulated by using the computed frequencies of the optimized geometrical configuration of the trimer in gas phase. The experimental FTIR spectrum for chitosan was obtained from a Bruker Alpha-T spectrometer.

Result and Discussion

The Optimized chitosan molecule (trimer) is shown in figure 2.
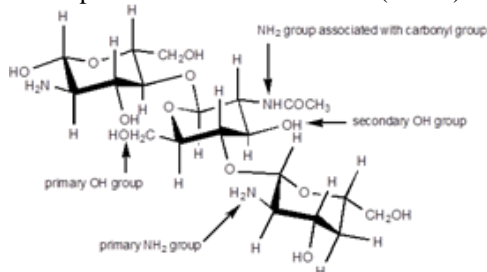

Figure 1: Possible metal binding sites of
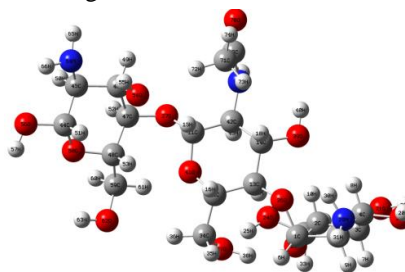
Figure 2: The Optimized chitosan molecule

chitosan.   with the labeled atoms (trimer)

It was clearly observed that the IR bands in simulated IR spectrum of optimized chitosan trimer (theoretical) show a similar pattern with those in FTIR spectrum of chitosan (experimental) for the range between 400 cm^{-1} and 4000 cm^{-1}. For instance, when the FTIR spectrum of chitosan (figure 3 (a)) measured in the 1590 cm^{-1} - 1800 cm^{-1} region is compared with computed IR spectrum of chitosan trimer (figure 3 (b)), it clearly indicates that the band patterns and their corresponding intensities of theoretically obtained IR spectrum are very much similar to that of experimentally obtained IR spectrum. Hence, it is clearly shown that simulated IR spectrum of chitosan by DFT calculations could be used to identify the vibrational bands in the close vicinity of metal binding sites and their corresponding vibrational modes. Therefore the vibrational assignment for the bands in the FTIR (experimental) could be easily obtained.
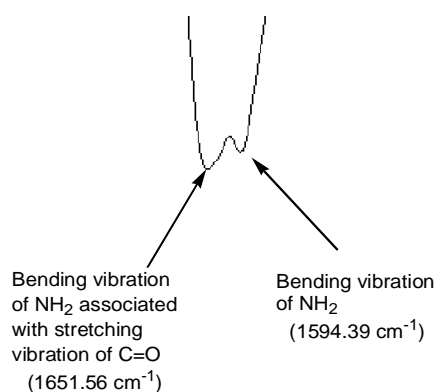
Bending vibration
of NH_2 associated
with stretching
vibration of C=O
(1651.56 cm^{-1})

Bending vibration
of NH_2
(1594.39 cm^{-1})

Bending vibration
of NH_2 associated
with stretching
vibration of C=O
(1793.50 cm^{-1})

Bending vibration
of NH_2
(1697.10 cm^{-1})

Figure 3 (a): IR bands in experimental
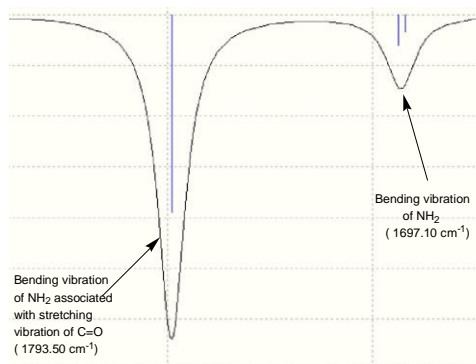spectrum in the region of 1590 cm^{-1} - 1800 cm^{-1}

Figure 3 (b): IR bands in theoretical spectrum
in the region of 1590 cm^{-1} - 1800 cm^{-1}

Experimental and computed IR frequencies of selected bands are shown in table 1 and their corresponding vibrational assignments were successfully determined by the use of simulated IR spectrum are also tabulated in table 1.

Table 1 - Experimental and theoretical frequency values of selected IR bands of chitosan and their corresponding vibrational assignments.

Theoretical frequency value / cm^{-1}	Experimental frequency value / cm^{-1}	Assignment
3439.99 - 3767.34	3425.10	Stretching vibration of NH_2 and OH
1697.10	1594.39	Bending vibration of NH_2
1091.52	1089.54	Stretching vibration of C-O
1793.50	1651.56	Bending vibration of NH_2 associated with stretching vibration of C=O

Upon binding of metal with chitosan, the IR of the bonds (IR bands) in the close vicinity of the coordination site will be significantly shifted when compared with metal-free chitosan as the metal binding affects the normal vibration scheme of chitosan due to the formation of new chitosan-metal bond. For instance, according to figure 4, the bending vibration band of chitosan at 1594.39 cm^{-1} was shifted to a higher frequency value upon binding of cadmium to chitosan indicating that

there is an interaction between the primary NH_2 group of chitosan and the cadmium. Hence, the actual coordination sites of metal, in the formed metal-chitosan complex could be cognized by identifying the IR bands which are significantly shifted upon metal binding. Therefore, this may serve as an identification tool for determining the structural assignment of the formed metal-chitosan complexes.
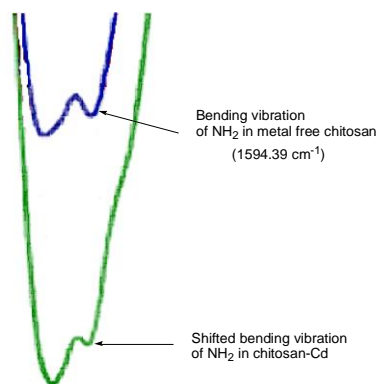

Bending vibration
of NH_2 in metal free chitosan
(1594.39 cm^{-1})

Shifted bending vibration
of NH_2 in chitosan-Cd

Figure 4: Experimental IR band shift of bending vibration of NH_2 of chitosan upon binding with Cd

Conclusion

By analyzing the theoretical IR spectrum of chitosan, the vibrational bands (bonds) in the close vicinity of the metal coordination sites and their corresponding vibrational modes could be clearly identified and hence those in the FTIR (Experimental) spectrum of chitosan could be correctly assigned. Further, the structural assignment of the formed metal-chitosan complex could be determined as there is a significant shift in the IR bands in the close vicinity of coordination sites upon metal binding. Hence this may serve as a diagnostic tool for determining metal binding preferences of bioadsorbents such as chitosan and might be other biological compounds.

References

Cahyaningrum, S.E., Herdyastuti, N. (2011). Sorption of Mg(II) and Ca(II) metal ions on chitosan-alginate membrane. Journal of Materials Science and Engineering. 1, 87- 92.

De Silva, S.M., Fernando, W.T.I., Kannangara, A.T., Ubesena, J.G.P.S., Rajapakse, C.S.K. (2014). Determination of heavy metal adsorption capacity of chitosan and removal of heavy metals from drinking water using chitosan. Proceedings of Third International Symposium on Water Quality and Human Health: Challenges Ahead, Postgraduate Institute of Science (PGIS), University of Peradeniya, Sri Lanka. pp. 37.

CuO free p-Cu$_2$O nano-surfaces prepared by oxidizing copper sheets with a slow heating rate exhibiting the highest photocurrent and the H$_2$ evaluation rate

U. S. Liyanaarachchi, C. A. N. Fernando
Department of Electronics, Faculty of Applied Sciences, Wayamba University of Sri Lanka, Kuliyapitiya, Sri Lanka

and

S. N. T. De Silva
Department of Biotechnology, Faculty of Agriculture & Plantation Management, Wayamba University of Sri Lanka, Makandura, Sri Lanka

Introduction

Among the various metal oxide materials for solar energy applications, p-type cuprous oxide (p-Cu$_2$O) is a promising non-toxic and low cost semiconductor with attracted attention for many decades (Mittiga *et al., 2006)*. It was reported that p-Cu$_2$O can be prepared by various fabrication processes such as thermal oxidation, electrochemical oxidation, chemical bath deposition and chemical vapor deposition. Low energy conversion efficiency of p-Cu$_2$O based solar energy conversion devices is due to the prevention of the photo-generated charge carrier separation in the micron–sized Cu$_2$O grains on the surface enhancing the recombination process. If the grains radius is reduced from micron to nano-size, the opportunities for recombination can be dramatically reduced enhancing the light absorption properties of the films. Therefore, the preparation of nano-crystalline Cu$_2$O thin films is a key factor to improve the performance of solar application devices without destroying the crystalline properties of the Cu$_2$O films. Hence, the present work is aim to fabricate CuO free nano-crystalline p-Cu$_2$O by thermal oxidation of copper sheets under maintaining slow heating rate for the first time. Structural and photoelectrochemical properties are also aimed to study.

Methodology

The outer layers of commercially available (99.99% purity) copper sheets 2cm×4cm were removed by sand papers and polished with Brasso Metal Polisher until obtaining a mirror like surface. Thereafter, polished copper sheets were washed with a surface detergent and distilled water several times. Well cleaned copper sheets were inserted into a Quartz Tube in a Cabolite-301 Tube Furnace opening both ends by filling normal air during the oxidation process. Initially a heating rate 10ºC/min was provided inside the furnace with copper sheets starting from the room temperature. After reaching 300ºC, 400ºC, 450ºC and 700ºC the temperature kept constant for 30min and then cooled down to room temperature. Experimentally that it was found that the 10ºC/min heating rate was the most suitable to fabricate mechanically stable p-Cu$_2$O on copper sheets. Samples prepared above 450 ºC temperature profiles did not produce mechanically stable Cu$_2$O films on copper sheets. Furnace temperature below 300ºC was not sufficient to oxidize copper sheets to form quality Cu$_2$O surfaces.Fig.2 shows the appearance of the Cu$_2$O films

prepared. Four different surface colors exhibited at each temperature profile expecting four different surface morphologies.

Result and Discussion

Fig.01 shows the diffuse reflectance spectra for the samples prepared from 300℃, 400℃, 450℃ and 700℃ temperature profiles. For the samples prepared from 300℃, 400℃ and 450℃ temperature profiles show absorption edges 630nm, 620 nm and 600nm, to the band gaps 1.98eV, 2.0eV and 2.1 eV due to band to band transitions of Cu_2O. Band gap 1.4eV for an absorption edge ≈850nm can be observed for CuO crystals prepared from 700℃ temperature profile. It should be mentioned that the absorption edges for Cu_2O corresponding to the 300℃, 400 ℃ and 450℃ temperature profiles cannot be observed clearly for the samples prepared at 700℃ temperature profile as shown. So that, it can be concluded the most light is absorbed by CuO regions than the Cu_2O regions for the samples prepared from 700℃ temperature profile.
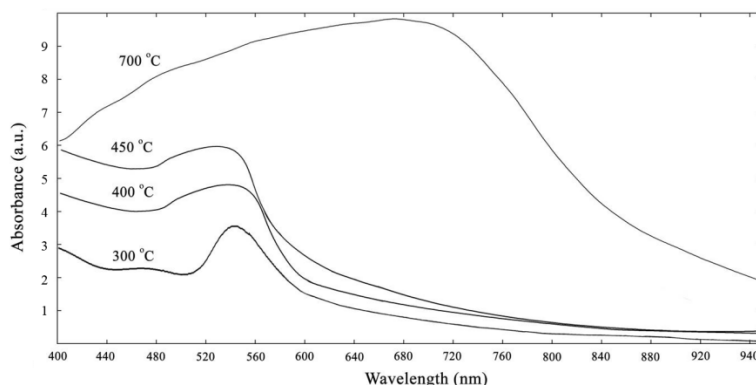

Figure01- Diffuse reflectance spectra of the p-Cu_2O thin films fabricated from 300℃, 400℃, 450℃ temperature profiles and p-CuO fabricated from 700℃ temperature profile

Table 01- Crystallite sizes estimated from XRD and AFM images prepared from 300℃, 400℃, 450℃ and 700℃ temperature profiles

	XRD (nm)	AFM (nm)
300 ℃	312.2	**308.9**
400 ℃	486.1	**488.3**
450 ℃	393.4	**395.1**
700 ℃	**320.7**	**322.3**

Table 01 shows the crystallite sizes estimated from XRD and AFM images obtained from samples prepared from 300℃, 400℃, 450℃ and 700℃ temperature profiles. It shows that the crystallite sizes obtained from both XRD and AFM are in good agreement of nano meter range.

According to figure 02 that the flat band potential for three samples are almost same ($\approx$+.53 vs Ag/AgCl). Here it is assumed that the flat band potentials are nearly equal to the valance band (VB) position of the samples prepared from each temperature profile. The H^+/H_2 (-0.61V vs Ag/AgCl at pH=7) and O_2/H_2O (+.62V vs Ag/AgCl at pH=7) were obtained from the literature (Nian *et. Al., 2008)*. It should be mentioned that the conduction band (CB) position of the samples prepared from 300ºC, 400ºC and 450ºC profiles is more negative than the H^+/H_2 redox level showing a favorable CB band position to reduce water. Highest H_2 evolution rate was observed for the Cu_2O thin films prepared from 450ºC temperature profiles in the presence of 1M Na_2SO_4 at -0.4V vs Ag/AgCl biased potential may be due to the more negative CB position as shown in Figure 02. Highest photocurrent ($\approx$ 10 mAcm^{-2}) was observed for sample prepared from 450ºC temperature profile under above experimental conditions is a remarkable finding.
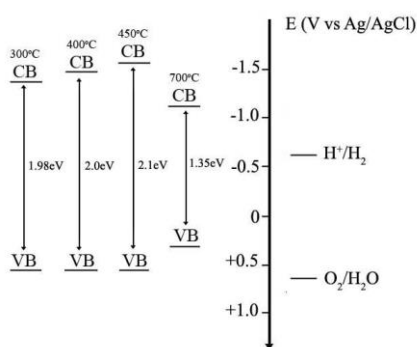

Figure 02- estimated band positions of nano-surfaces, H^+/H_2 and O_2/H_2O redox levels prepared from 300ºC, 400ºC, 450ºC and 700ºC temperature profiles

Conclusions

p-Cu_2O films prepared from 300ºC, 400ºC and 450ºC temperature profiles with 10ºC/min slow heating rate produced single phase Cu_2O nano-crystals and the films fabricated from 700ºC temperature profile coexist Cu_2O and CuO two phases. A blue shift of the band gap of Cu_2O was observed for the Cu_2O fabricated from the 450ºC temperature profile with compared to the Cu_2O films fabricated from 300ºC and 400ºC temperature profiles may due to the quantum confinement effect of the crystal sizes as exhibited from AFM micrographs. The highest H_2 evolution ($\approx$ 6.2 Moles l^{-1}min^{-1}) and photo-current enhancement ($\approx$ 10 mAcm^{-2}) from p-Cu_2O nano-surfaces fabricated from 450ºC temperature profile was observed with compared to the recent studies presented by Gratzel and co-workers (Paracchino *et al.*,2011) and the similar systems reported in the literature.

References

Mittiga A., Salza E., Sarto F., Tucci M. and Vasanthi R.,(2006), *Appied Physics Letters*, 88:163502

Nian J., Hu C. and Teng H., (2008), *International Journal of Hydrogen Energy,* 332897

Paracchino A., Laporte V., Sivula K., Grätzel M. and Thimsen E., (2011). Highly active oxide photocathode for photoelectrochemical water reduction. *Nature Materials,* 10:456-461

Toxic Metal Absorptivity to Agriculture Soil

M.A.N Chamara*, J.T. Cooray and A.N.B. Attanayake

Faulty of Science &Technology, Uva Wellassa University, Badulla, Sri Lanka

Introduction

Soil contamination has increased by several folds within the recent past due to various man made activities. Various types of toxics involve in the processes of making contaminated soil profiles. There are many toxic metals and chemical complexes which contaminate soils. When toxic agents contact with soils they may absorb or adsorb in to the soil structure depending on their structural and physical properties. One of the major sources of contaminant is agrochemicals. Due to expansion of agricultural practices and over use of agrochemicals (pesticides, weedicides, insecticides, fungicides and others) the effect has become adverse.

Sri Lanka is covered with versatile range of soils with highly contrast physical properties. In this study, soil samples from different agricultural areas in Badulla district have been used to determine their quantity of toxic metal absorptivity quantitatively.

Method

Five areas were selected where there are many types of agricultural activities. Uncontaminated samples were collected from these farms (Mirigama, Passara, Badulla Bandarawela and Welimada). Soil properties like moisture content, soil pH, bulk density, hydraulic conductivity, soil porosity were studied in order to categorize the soil types.

Soil columns were made for these samples and metal absorptivity was studied by adding *Roundup* pesticide (which is heavily used agrochemical in the area). Concentration of the agrochemical was kept at its normal dosage. Original agrochemical was fully studied with ASS to identify the containing metal ions and the obtained leachates were also measured for the same set of metal ions to confirm their soil absorptivity under specific time period.

Obtained AAS results interpreted to identify the correlations between soil properties and toxic metal absorptivity.

Results

Table 01: The soil properties of collected samples

sample	pH	Moisture content	Bulk density	porosity	Hydraulic conductivity
A	4.18	25.975	1.12	57.7358	0.131408
B	4.77	2.749	0.84	68.3018	0.408656
C	4.05	11.82	0.74	72.0754	0.277594
D	4.43	5.222	0.86	67.5471	0.366963
E	4.48	12.758	0.76	71.3207	0.0116
F	4.56	12.76	0.82	69.0566	0.308462
G	5	0.562	0.64	75.8490	0.2583
H	5.07	0.513	0.72	72.8301	0.511017
I	4.13	7.645	0.68	74.3396	0.278002
J	4.47	5.229	0.7	73.5849	0.172283
K	5.84	34.976	1.12	57.7358	0.421605
L	4.42	17.467	0.98	63.0188	0.524233
M	5.62	13.258	0.82	69.0566	0.182757
N	6.69	11.842	0.96	63.7735	0.38114
O	5.7	8.886	0.82	69.0566	0.149535

Soil properties like soil Ph, soil moisture, soil bulk density, soil porosity, soil hydraulic conductivity were measured. Then toxic metal absorbance to soil was measured by AAS and results are graphically shown here. Then it was analyzed whether there is any relationship between soil properties and toxic metal absobvity.
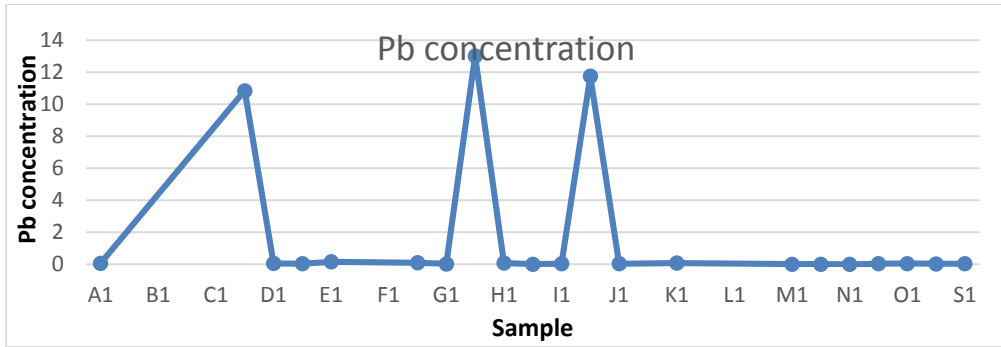
Figure 01 : Pb concentration variation of samples.

Pb concentration of samples varies as G > sample I > sample C

Three samples are in acidic state. Acidic environment is better for Absorption of Pb. Moisture content does not affected to the absorption of Pb. Lower bulk densities are preferred for absorption of Pb. High porosity is better for Pb absorption. Hydraulic conductivity also does not affect to the absorption of Pb. Other samples do not show a Pb concentration because their absorbance is less than 0.001.
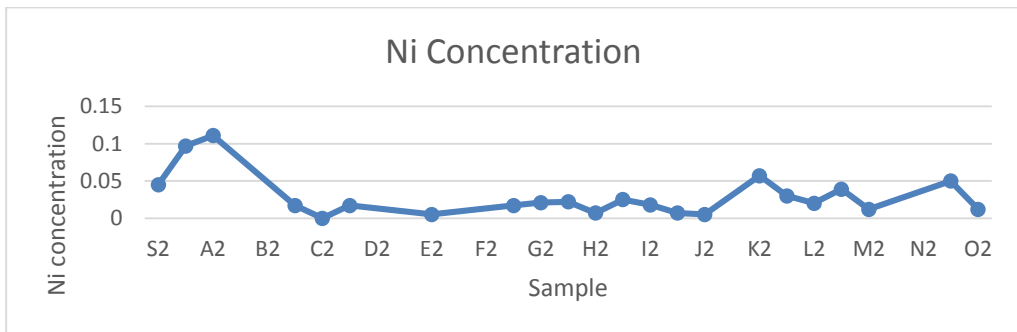
Figure 02 : Ni concentration variation of samples.

Ni concentration of samples varies as, A> Sample k > sample O

Acidic environment is preferred for the Ni absorption. Moisture content does not effect to the Ni absorption. High bulk density is better for Ni absorption. Low porosity is better for Ni absorption. Hydraulic conductivity does not much affected to the absorption of Ni.
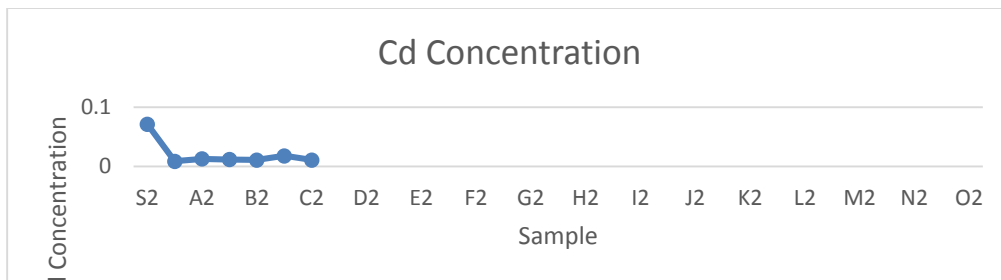
Figure 03 : Cd concentration variation of samples.

Cd is present in sample A,B and C in little amounts. There is no Cd in other samples because their Cd absorbance is less than 0.001
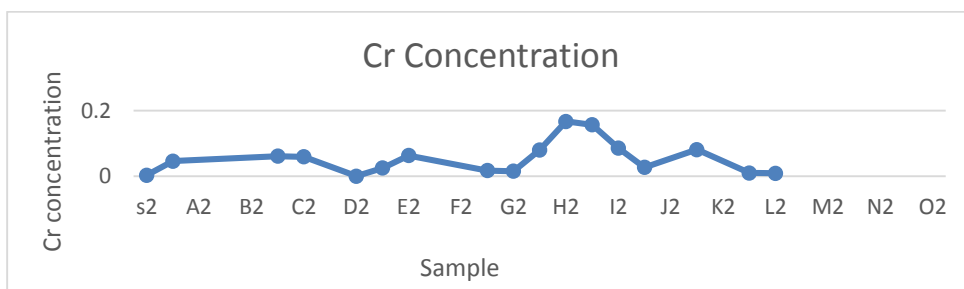

Figure 04 : Cd concentration variation of samples.

Cr concentration of samples varies as, sample H> sample I > sample k

Acidic environment is preferred for the Cr absorption Moisture content does not affect to the absorption of Cr Bulk density, porosity and hydraulic conductivity do not effect to the absorption of Cr

Conclusion

According to the obtained results soils with higher organic content have absorbed higher amount of toxic metals. Soil pH and hydraulic conductivity do not affected significantly in the absorptivity of metals.

In this investigation was used agrochemical in small amount and the cause of agricultural field have accumulated various large number of agrochemical due to the usage of agro chemicals as type of insecticides, pesticides, weedicides and fungicides. These types of agrochemicals are accumulated during the last number of years. That caused to the agricultural soils were contaminated by significant amount of toxic including toxic metals which accumulated toxics were finally entered to the ground water and this cause to contaminate the ground water and the environment related to it.

References

Trace Metal Concentration in Crops and Soils Collected from Intensively Cultivated Areas of Sri Lanka was studied under laboratory conditions by HMP Lakmalie Premarathna GM Hettiarachi and S P Indrarathne.

W.V.P. De Soysa, A.S. Amarasekara (1994).Absorption of the pesticide propanil on agricultural waste products.Department of chemistry, University of Colombo.

Manar Ahmad Attaallah (2011). The Kinetic Study of Glyphosate Leachate in Palestinian Soil at Different Concentrations, Degree of Master of Science in Chemistry, Faculty of Graduate Studies, at An-Najah National University at Nablus,Palestine.

Synthesizing Electro - conductive grease using graphite

W.A.P.P Christopher*, J.T. Cooray and A.N.B Attanayake
Faculty of Science and Technology, Uva Wellassa University of Sri Lanka

Introduction

Graphite as we all know is well renowned for its ability to conduct electricity as well as its lubricant nature. The carbon atoms in graphite are sp^2 hybridized. Each carbon atom bonds with three other carbon atoms via the three sp^2 hybridized atoms to form a sheet of carbon atoms lying in a hexagonal pattern or a honey comb structure and carbon atoms are bound together by strong covalent bonds. And each of these sheets of carbon is bound together by weak van der Waals bonds. The fourth electron in a p orbital is left free and its these electrons that contribute towards the electrical conductivity of graphite. Grease is a semi solid lubricant widely used in the industrial world to reduce ware and tare. Grease is made of three principal components known as a base oil, thickener and additives. Thus combining graphite with grease would preferably transfer the electro-conductive nature of graphite to grease forming an electro-conductive grease.

Usage of such a product would be, grounding static discharges, providing electrical continuity between irregular or pitted surfaces, ensuring electrical contact between loose or vibrating parts and small gaps, application to ball bearings in computer equipment where it allows static discharge to pass through the bearing instead of building up and arcing. Synthesizing such a graphite based grease product was the main objective of this study.

Materials and methodology

Natural vein graphite was used to make graphite powder under 75 microns. Basic grade grease was used as the substrate. Different weight ratios of both graphite and grease were mixed by blending to generate the sample series. The samples were tested for electrical conductivity using the impedance analyzer. A standard cell was made to hold the sample. The conducting length was kept to a minimum assuming that in real world applications (12 millimeters).

The cell electrodes were designed in such a manner that two over rings were placed to ensure that the effective conducting length was kept constant throughout the sample series tested. Three measurements were taken with each generating a graph of imaginary part of impedance versus the real part of it. And the resistance of the sample was determined by the point where the curve seemed to make contact with the x axis of the graph. And the capacity of the particular sample can be determined by finding out the frequency of the peak point of the semicircle.

$$2\pi f = \omega \;\ldots\ldots\ldots\ldots \; (3)$$
$$\omega = \frac{1}{R\,c} \;\ldots\ldots\ldots\ldots \; (4)$$

Thus,

$$2\pi f = \frac{1}{Rc}, \;\ldots\ldots\ldots \; (3)\ \&\ (4).$$
$$c = \frac{1}{2\pi f R}$$

Where,

c- Capacity, f- Frequency of the peak point of semicircle, R- Resistance of the peak point of semicircle.

Results and discussion

The samples show a near linear variation of both characteristics of conductivity and capacity. But the final sample containing 35% graphite with 65% grease shows a significant elevation in both conductivity and capacity. With a conductivity value of 4.2008 x 10^{-5} S cm^{-1} this particular sample is in the region of semiconductors with respect to conductivity.
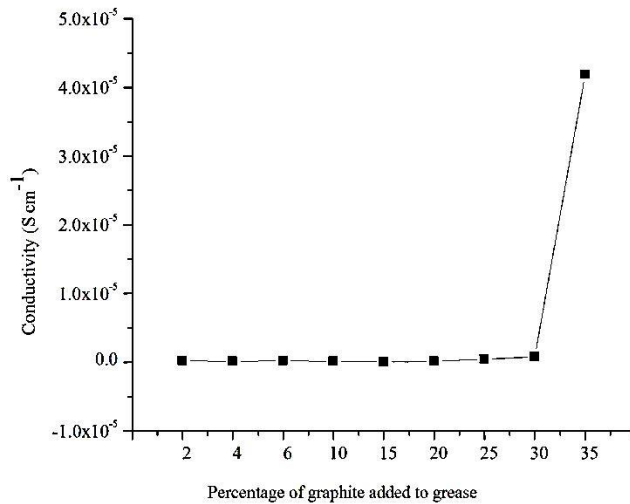

Figure 01: Conductivity variation of the sample series at room temperature

The figure 01 indicates a clear and significant elevation of conductivity for the sample containing 35% graphite with 65% grease while the preceding samples are scattered very closely with respect to their conductivity values. And the capacity of the samples vary almost linearly with the amount of graphite in them and shows a rapid increase when it come to the sample with 35% graphite according to figure 2 below. The capacity values change from Pico farads to Nano farads.
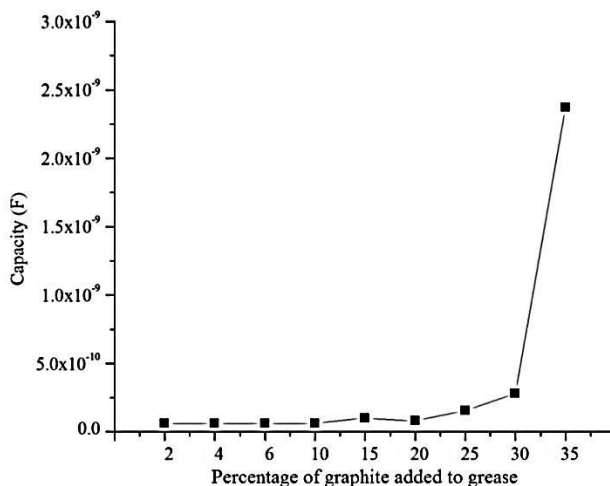
Figure 02: Capacity variation of the samples in room temperature

Conclusions

The samples show a near linear variation of both characteristics of conductivity and capacity. But the sample containing 35% graphite with 65% grease shows a significant elevation in both conductivity and capacity. With a conductivity value of 4.2008 x 10^{-5} S cm$^-$1, which puts it in the region of semiconductors with respect to conductivity ("Electrical Conductivity: Range of Conductivity." *Encyclopaedia Britannica*. N.p., n.d. Web. 10 July 2014). And all the samples resembled a parallel plate capacitor connected to a resistance parallel, implying that they had a capacity to store static charges. And all these characteristics are in favor of the product with respect to its uses.

References

Encyclopaedia Britanica (2014), <u>Electrical conductivity: range of conductivity</u>. Retrieved July 10, 2014, from the World Wide Web:
http://www.britannica.com/EBchecked/media/139/Typical-range-of-conductivities-for-insulators-semiconductors-and-conductors.html

Estimating the magnetite content of the Southern part of Eppawala Phosphate Deposit and its parent rock

H.P.V.H.Erandi , A.N.B. Aththenayake
Faculty of Science and Technology, UvaWellassa University of Sri Lanka

N.D.Subasinghe
Institute of Fundamental Studies, Kandy, Sri Lanka


and

W.K.B.N. Prame
Geological Survey and Mines Burro, Sri Lanka

Introduction

Phosphorus is one of most important plant nutrients because its function cannot be performed by any other nutrient. Phosphate fertilizer is mainly produced from the natural phosphate rocks worldwide. Phosphate deposit at Eppawala is one of the most economically valuable mineral deposits in Sri Lanka. It contains up to 42% of P_2O_5 while the citric acid solubility of various components varies from 4% to 6%. Due to strong weathering of apatite-bearing parent carbonatite rock, an economically valuable secondary phosphate deposit has formed (Subasinghe, 2013). Former studies revealed that iron leaching from weathering parent rock played an important role in fixing phosphate and formation of secondary deposit through in-situ diagenesis (Subasinghe, 2012). Source of iron is assumed to be magnetite and other iron bearing minerals. To reap grater benefits from the deposit it is necessary to produce value added products such as triple super phosphates. Due to considerable amount of iron impurities from magnetite and other iron baring minerals, the production of super phosphate may pose some difficulties at industrial level. The objective of this study is to develop a methodology to estimate the magnetite, the main iron-bearing mineral, in the phosphate ore.

Methodology

Northern Deposit   Southern Deposit
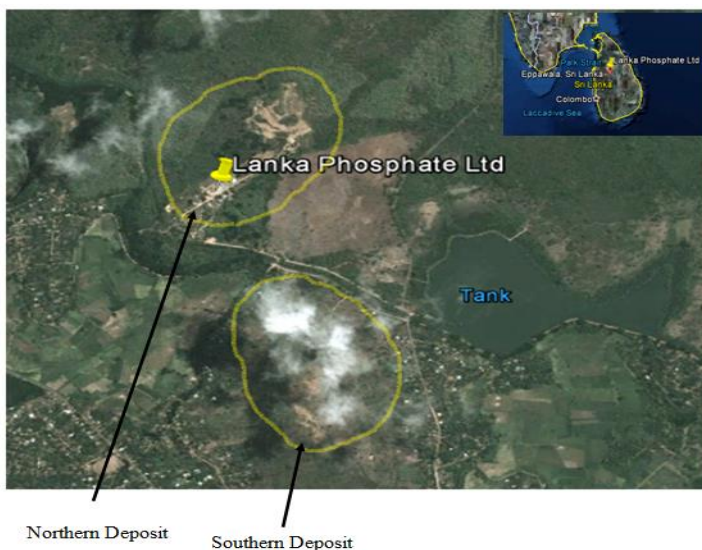
Depending on the extent and exposure of the deposit two specific areas (Southern part and Northern part) were identified for the sample collection. Due to relative scarcity of magnetite in the northern deposit, seventy samples were collected randomly from only southern deposit. Then suitable twelve samples were selected for thin section making and ten samples were selected for XRF analysis. Then representative sample from each sample was selected and they were ground to pass 600 µm sieve. Then the fraction between 250 µm to 600 µm was taken and washed and dried. Then 25 g of representative sample again was taken for magnetic separation. At the first magnetite setting (0.125 A) was set and magnetites in the representative samples were separated by free fall mode. Then all other magnetic minerals in the representative sample was separated from the sample (1.2 A) by free fall mode. Samples powdered by disc mill were used to XRF analysis. Powder method was followed to analyze samples in XRF. Hand held XRF at GSMB was used to analyze samples. Thin section preparation of selected samples was done and they were analyzed by petrographic microscope at GSMB.

Result and Discussion

The average percentage of magnetite in primary rock is 0.1% and in the secondary phosphate deposit is 0.21%. The average percentage of magnetic minerals in the secondary deposit is 20.21 % and parent rock is 2.78%. Magnetic susceptibility data, XRF data and results from thin section analysis are not comparable with results gained from magnetic separation method. That means magnetite is not the only source of iron or magnetite is not having theoretical composition. During weathering processes, Fe^{3+} has greater tendency to accumulate in regolith. Because of its mass transfer coefficient is -1 that means element is completely lost from the parent rock (Hewawasam, 2013).
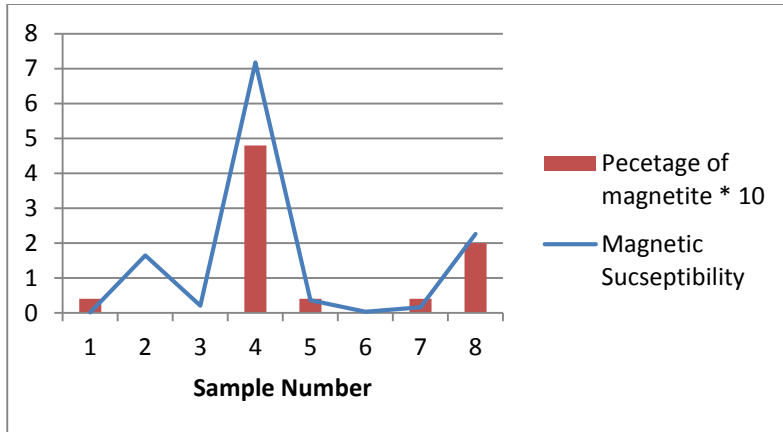
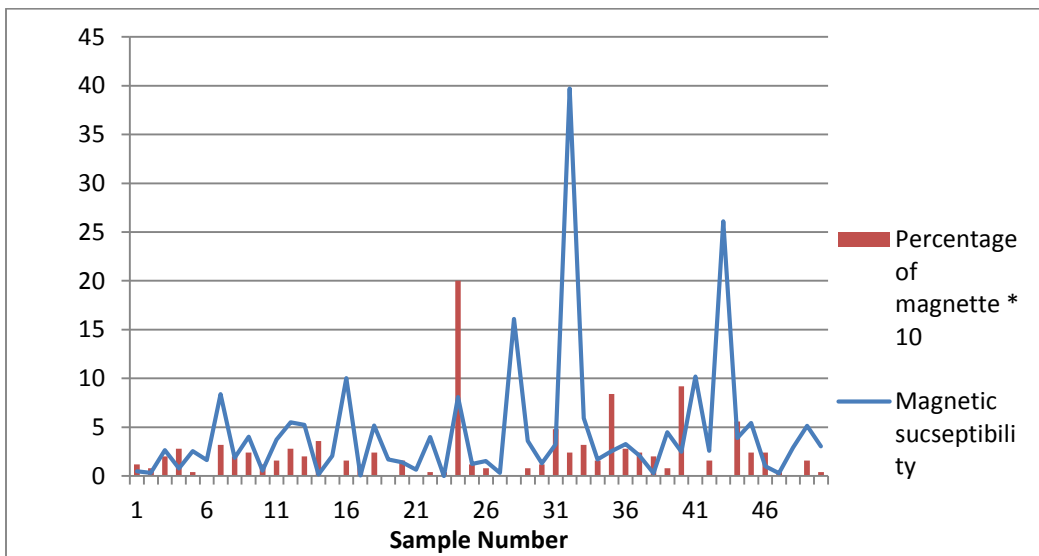Figure 6 : Comparison between magnetite percentage and magnetic susceptibility of parent rock

Figure 7 : Comparison between magnetite percentage and magnetic susceptibility of parent rock

Conclusions

According to data gathered from several methods described above it is clear that the magnetite percentage of the parent carbonatite rock and secondary phosphate rock of the southern part of the phosphate deposit at Eppawala is considerably very low. But percentage of all magnetic mineral is raised up to considerable amount. So it is clear that there are several magnetic as well as iron bearing minerals in both secondary deposit and parent rock. Rapid weathering of magnetite and other iron bearing minerals may be the reason for the percentage difference of magnetite and magnetic minerals in both parent rock and secondary deposit.

Acknowledgement

References

Hewawasam, T. (2013). Tropical weathering of apatite bearing rocks of Sri Lanka: Major element behavior and mineralogical changes.Journal of the Geological Society of Sri Lanka 15, 31-46.

Subasinghe, N.D. (2013). Observations and interpretations on past microbial activities at Eppawala phosphate deposit, Journal of the Geological Society of Sri Lanka 15, 99-110.

Subasinghe, N.D. (2012). Electron microscopic studies on phosphate binding processes in the presence of iron. Advanced Materials Research Vols. 343-344, 307-311